

Propulse NTNU - Project Bifrost

Team 18 Project Technical Report 2023 European Rocketry Challenge

(See Section 12 for author list)



Norwegian University of Science and Technology (NTNU), 7031 Trondheim, Norway

Department of Electronic Systems

Department of Energy and Process
Engineering

Department of Engineering Cybernetics

Department of Computer Science

Department of Physics

Department of Mechanical and
Industrial Engineering

Department of Structural Engineering

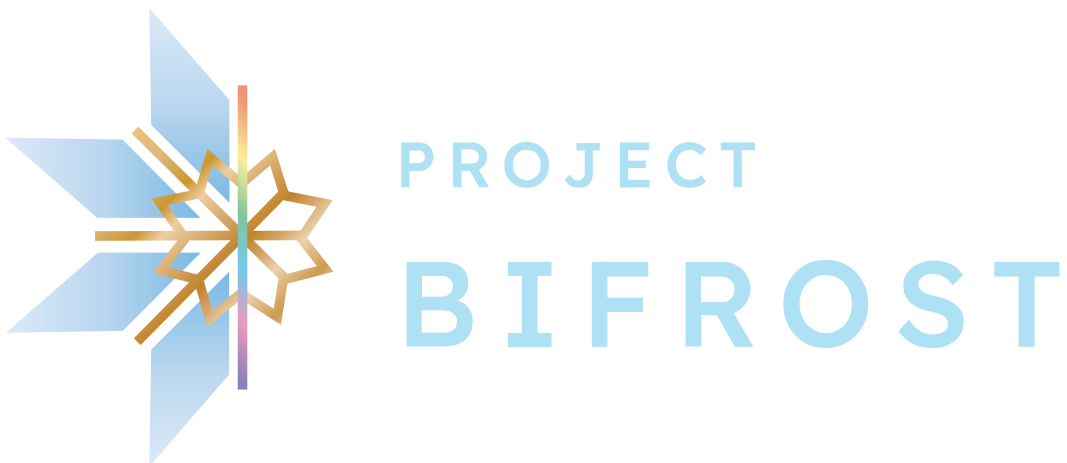
Department of Materials Science and
Engineering

Department of Economics

Department of Language and Literature

Abstract

Propulse NTNU presents Project Bifrost, a bi-propellant liquid rocket that will represent Norway in the 2023 European Rocketry Challenge. Bifrost is propelled by Propulse's first SRAD propulsion system that delivers 24750 Ns of impulse and has a target apogee of 3000 m. The project is a large technological leap towards the organization's overarching goal - to reach space with a self-developed liquid-fueled rocket. By combining new systems with flight-proven designs, the project aims at creating a reliable and capable platform for liquid rocketry, all-the-while enriching the engineering capabilities of the student members. Bifrost features load-bearing fiber composite airframe sections and four carbon fibre fins with a modified clipped delta shape. Hatches in the aft airframe section allow for access to the internal systems during assembly and pad procedures. For recovery, Bifrost uses a dual deployment system with in-house manufactured drogue and main parachute. Deployment of both parachutes is performed by flight-proven SRAD systems. The main aspects of Bifrost's avionics system are the SRAD Flight Computer and a Engine Controller Unit that control the recovery and propulsion systems respectively. All telemetry, including a on-board video feed, is transmitted live through the ground station throughout the entire flight profile. Bifrost will carry a 4 kg 3U cubesat payload built by the student organization Orbit NTNU, and is a structural model of the BioSat satelite project.



Contents

1	Introduction	1
1.1	Organization	1
1.2	Project Bifrost	1
1.3	Stakeholders	1
2	Overview of mission operations	2
3	System architecture	3
3.1	Overview	3
4	Propulsion system overview	4
5	Thrust chamber	5
5.1	Combustion chamber	5
5.1.1	Theoretical performance using NASA CEA	5
5.1.2	Inner chamber and nozzle	6
5.1.3	Cooling channels	6
5.2	Injector	7
5.3	Bulkhead	8
5.4	Sealing methods	9
5.5	Ignition system	9
6	Feed system	10
6.1	System function and system overview	10
6.2	Safety Features	10
6.3	P&ID	11
6.4	Propellant storage	12
6.5	Pressurising system	13
6.6	Flow control	14
7	Outer structure	15
7.1	System function and system overview	15
7.2	Nose Tip	15
7.3	Nosecone	15
7.4	Forward Airframe	16
7.5	Aft Airframe	17
7.6	Launch lugs	17
7.7	Hatches	18
7.8	Fins and fin brackets	18
7.9	Boat Tail	19
7.10	Composite validation	19
7.11	Flight validation	20
8	Inner structure	22
8.1	System function and system overview	22
8.2	Payload module	22
8.3	Radax joint	23
8.4	Recovery and avionics module	24
8.5	Aft end	26
8.5.1	Pre-engine	26
8.6	Connections to airframe	27
9	Recovery	29
9.1	System function and overview	29
9.2	Separation system	29
9.3	Deployment system	31

9.4	Main chute release system	32
9.5	Deployment forces	34
10	Avionics	35
10.1	System Overview	35
10.2	COTS Avionics System	35
10.3	SRAD Electrical System	37
10.3.1	Flight Computer	37
10.3.2	RF System	38
10.3.3	Engine Control Unit	38
10.3.4	Arming System	39
10.3.5	Camera System	40
10.3.6	Power System	40
10.4	SRAD Software System	41
10.4.1	Flight Computer Software	41
10.5	Engine Control Unit Software	43
10.6	SRAD Ground Station	43
10.6.1	Ground Station Hardware	43
10.6.2	Ground Station Software	43
10.6.3	Ground Station Tracker	43
11	Payload	45
11.1	Introduction	45
11.2	Payload structure	45
11.3	BioBox	45
11.4	Electronics	45
12	Conclusions	46
A	System data	49
B	Projects and test reports	52
C	Projects and test reports	209
D	Risk assessment	216
E	Assembly, pre-flight, and launch checklist	227
F	Engineering drawings	253
G	Deployment configuration	301
H	Ground station system design	309
I	Software system design	345
J	Electrical system design	381
K	Propulsion system design document	422
L	Additional tests	480
M	Calculations and analysis	488
N	Trajectory simulation & CFD Bifrost	555
O	Propulsion avionics	567

List of Figures

1	Flowchart of the Propulse NTNU CONOPS for Bifrost.	2
2	The Bifrost rocket	3
3	Inner structure of the Bifrost rocket	3
4	Render of aft CAD model	4
5	Combustion chamber during hot-fire testing	5
6	Performance values shown with varying OF-values ranging from 3-4.	5
7	Profile of the combustion chamber walls and cooling channels.	6
8	Machine drawing excerpt of the injector plate.	7
9	Injector plate mounted to bulkhead.	8
10	Mating surface of the combustion chamber, showing the circle of cooling channels.	8
11	Bulkhead with O-rings.	9
12	Assembled chamber mounted to test bench.	9
13	Igniter mount with shield	9
14	CAD of feed system.	10
15	CAD of the coaxial propellant tank.	12
16	CAD of pressurization module. Not all tubing is shown due to visibility.	13
17	CAD of main valve assembly including V-port ball valve, servo motor, and actuator mounting bracket.	14
18	Full outer overview	15
19	Nosetip overview	15
20	Nosecone model	16
21	Lower Hatch	18
22	Upper Hatch	18
23	Exploded view boat tail - with brackets and fins	18
25	Stability of the rocket from off rail to separation.	21
26	Overview of related inner structure	22
27	Assembled payload module	22
28	Exploded view of payload module	22
29	Exploded view of assembled radax joint	23
30	Section of the joints	23
31	Bare version of the recovery and avionics module	24
32	Recovery and avionics module with components	24
33	Mounting plate	24
34	Heated insert	25
35	Vibration dampening standoff	25
36	runcam	25
37	Overview of the nitrogen module	26
38	Pre-engine module	27
39	FEA analysis, VonMises(stress)	27
40	Each arrow marks a hole, and every arrow on the upside marks ø4.2mm in the airframe.	27
41	Recovery system overview.	29
42	Separation system overview.	29
43	The filling valve is located 1.7 m away from the bottom of the boat tail, behind a hatch.	30
44	Flight phases and altitude over time (left), velocity over time, note $t = 0$ is apogee here (right).	31
45	Deployment configuration.	32
46	A tennis ball used on project Stetind (left) and leather used for project Birkeland (right).	32
47	Overview of MCRS.	32
48	MCRS locked position (left), MCRS actuated (right). Note that one of the two servos is hidden to display the mechanism more clearly.	33

49	Overview of COTS avionics system.	35
50	Simplified SRAD electrical system overview.	36
51	Rendering of the Flight Computer.	37
52	Rendering of the Engine Control Unit.	38
53	FC FSM	42
54	Overview of BioSat and included sub-systems	45

List of Tables

3	Bifrost main parameters.	3
4	Propulsion main system parameters.	4
5	Identified OF and calculated performance values for maximum C*.	6
6	Combustion chamber main parameters.	6
7	Cooling channel dimensions for chamber, throat and nozzle.	7
8	Injector parameters for oxidizer and fuel. Tank pressure is 40 barg and combustion chamber (nominal) pressure is 20 barg.	8
9	Coaxial tank design values.	12
10	Details on COTS pressurant COPV.	13
11	Pressure regulator details for Tescom 44-1365-9082-002.	13
12	Overview of all valves in the feed system.	14
13	Parts, their incident forces, and the resulting safety factor after composite analysis.	20
14	Important flight values.	20
15	Results from FEA analysis on forward- and afr radax joint	23
16	Results FEA	27
17	Summarized results from FEA	34
18	Overview COTS components and experienced load.	34
19	COTS battery system specifications	35
20	COTS component overview.	36
21	Flight computer module functions.	37
22	Overview of antennas used	38
23	ECU module functions.	39
24	Actuators used in the propulsion system.	39
25	Sensors used in the propulsion system.	39
26	Camera specifications	40
27	Battery specifications.	40
28	Regulators used.	41
29	Flight Computer tasks	41
30	Groundstation functions	43

Abbreviations

EuRoC	–	European Rocketry Challenge
COTS	–	Commercial Off The Shelf
SRAD	–	Student Researched and Developed
DTEG	–	Design, test and evaluation guide [1]
R&R	–	Rules and requirements [2]
FEA	–	Finite element analysis
PV	–	Pressure vessel
CFD	–	Computational fluid dynamics
PCB	–	Printed circuit board
GNSS	–	Global Navigation Satellite System
NTNU	–	Norwegian University of Science and Technology
PBSS	–	Pressure based separation system
EuRoC	–	European Rocketry Challenge
OR	–	Open Rocket
FSM	–	Finite state machine
AoA	–	Angle of Attack
MEKF	–	Multiplicative Extended Kalman Filter
CNC	–	Computer numerical control
AGL	–	Above ground level

Nomenclature

A	–	Area
A_P	–	Projected Area
a	–	Average Attraction Between Particles
b	–	Volume Excluded by a Mole of Particles
C_D	–	Drag Coefficient
CG	–	Center of Gravity
CP	–	Center of Pressure
D	–	Maximum Diameter
d_i	–	Distance between CG of component i and rocket nose tip
F	–	Force
F_D	–	Drag force
$F_{D,\text{aft}}$	–	Drag force on aft airframe
$F_{D,\text{forward}}$	–	Drag force on forward airframe
g	–	Gravitational Acceleration
m	–	Mass
P	–	Pressure
q_∞	–	Dynamic Pressure
R	–	Universal Gas Constant
ρ	–	Density
ρ_∞	–	Freestream Density
α	–	Angle of Attack
β	–	Oblique Shock-wave Angle
σ	–	Stress
T	–	Temperature
V	–	Volume
V_∞	–	Freestream Velocity
v	–	Velocity
W_t	–	Total Rocket Weight
W_i	–	Component Weight

1 Introduction

1.1 Organization

Propulse NTNU is a volunteer student organization that provides students with knowledge and engineering experience through the design, production, and launch of sounding rockets. The organization is currently working on two projects: Project Bifrost, and an in-house trajectory simulator, Penumbra. These projects are the stepping stones toward our long-term goal of reaching space. All aspects of the organization are run entirely by students, with no influence by the university other than monetary support. Propulse NTNU currently has 66 active members and 15 mentors from 6 different faculties. The following seven disciplines ensure that all aspects of the project development run smoothly: Avionics, Propulsion, Mechanical, Marketing, Business, the Board and Mission Control. The non-technical disciplines support organizational growth and prosperity, whilst the technical disciplines develop the rocket.

1.2 Project Bifrost

Project Bifrost is the 5th rocket developed by Propulse NTNU since it's founding in 2018. Bifrost is propelled by Propulse's first SRAD propulsion system - a bi-propellant liquid engine that delivers 24750 Ns of impulse, enough to lift the 80 kg rocket to a target apogee of 3000 m. The project is a large technological leap towards the organization's overarching goal of reaching space with a self-developed liquid-fueled rocket. By combining new systems with flight-proven designs, the project aims to create a reliable and capable platform for liquid rocketry while enriching the engineering capabilities of the student members.

The main objectives of the project are as follows:

1. Launch an SRAD bi-propellant liquid rocket by 2024
2. Increase aerospace interest and expertise in Norway
3. Strengthen the bond to Orbit NTNU

1.3 Stakeholders

The primary stakeholders in the project are all team members. European Rocketry Challenge (EuRoC) establishes several requirements for the project. At the same time, our sponsors and the Norwegian University of Science and Technology (NTNU) have contributed to the project through expertise, production, and funding. The organization categorizes the 41 sponsors through the levels Platinum, Gold, Silver and Supplier/Supporter by contribution value. The platinum sponsors are Fieldmade and PLM Group. The gold sponsor is Radioror Communications. The silver sponsors are GKN Aerospace, Swagelok Norway, Windtec, Nippon Gases, FFI, 4test, Inission Løkken, EmLogic, NCAB Group, Nammo and NTNU Faculty of Engineering. The remaining sponsors are suppliers or supporters.

2 Overview of mission operations

In alignment to achieve a successful launch, Propulse has outlined a Concept of Operations. The launch procedure for the rocket Bifrost comprises six core phases: Assembly, On-Pad Assembly and Arming, Propellant Filling, Launch Window Initiation, Flight, and Recovery. It is essential to note that this Concept of Operations presupposes the successful completion of the rocket's assembly, ensuring a plug-and-play readiness upon arrival at the launch site. An overview of the concept of operations can be seen in Figure 1.

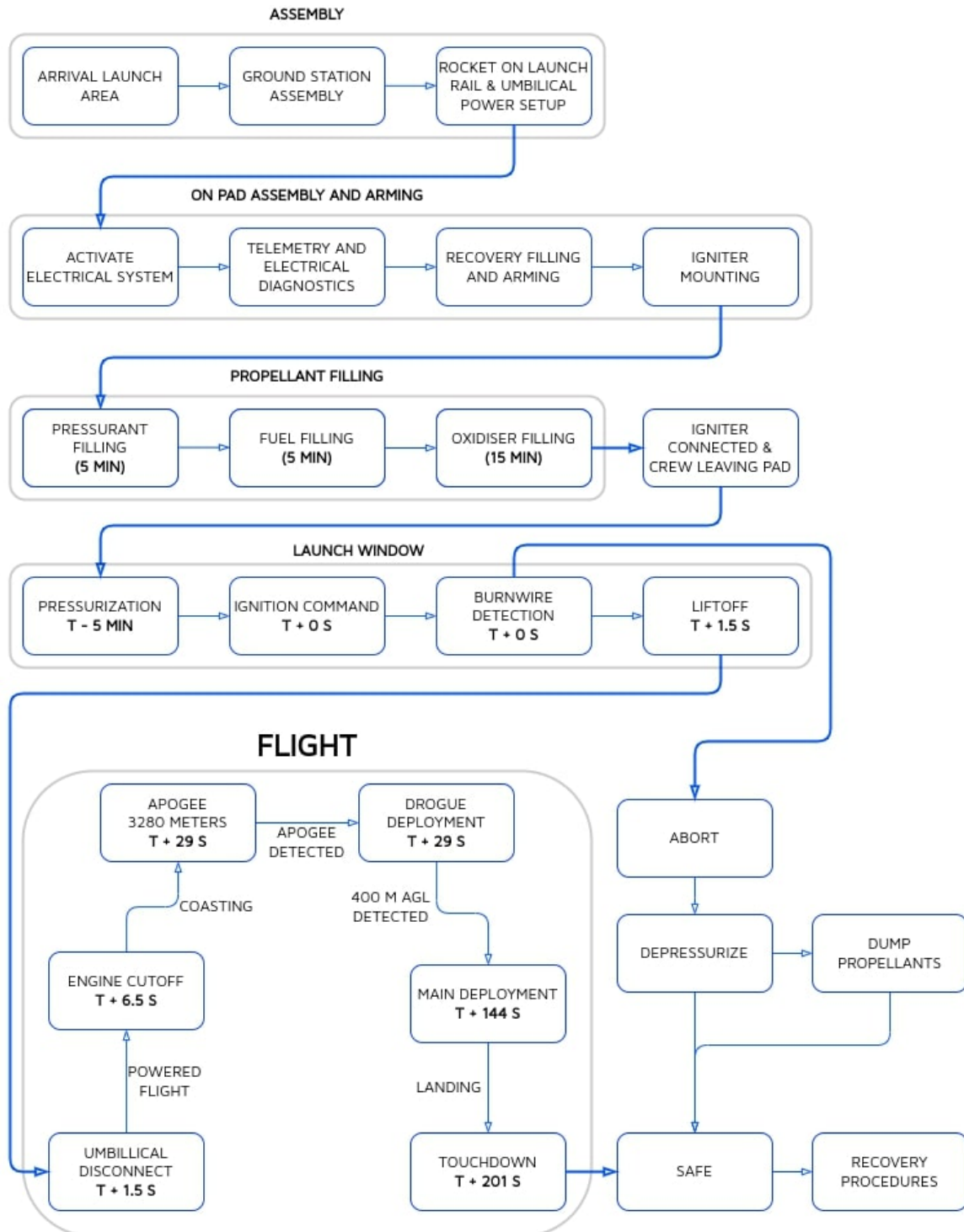


Figure 1: Flowchart of the Propulse NTNU CONOPS for Bifrost.

3 System architecture

3.1 Overview

Bifrost is a 4.7 meter tall rocket weighing 79.8 kg (wet), propelled by an SRAD bi-propellant liquid engine that delivers 24750 Ns of impulse. The target apogee is 3000 m above ground. A brief overview of the physical characteristics of Bifrost is given in Table 3. The value or type of the parameters have been influenced by a combination of self-imposed requirements and the requirements described in the DTEG [1]. Furthermore, the specific values are a result of simulations using the in-house simulator, Penumbra, and OpenRocket.

Table 3: Bifrost main parameters.

Parameter	Value/Type
Length	4.7 m
Airframe width	202 mm
Dry mass	65.7 kg
Wet mass	79.8 kg
Target apogee	3000 m
Propulsion system	Bi-propellant liquid engine
Propellant feed architecture	Active pressure-fed
Max thrust	4500 N
Burn time	5.5 s
Total impulse	24 750 Ns



Figure 2: The Bifrost rocket



Figure 3: Inner structure of the Bifrost rocket

4 Propulsion system overview

The propulsion system for Bifrost is an SRAD bi-propellant pressure-fed liquid rocket engine. It uses liquid nitrous oxide (N_2O) as oxidiser and ethanol (C_2H_6O) as fuel. It is actively pressurized using gaseous nitrogen (N_2).

Table 4: Propulsion main system parameters.

Parameter	Value	Unit
Average thrust	4500	N
Burn time	5.5	s
Total impulse	24 750	Ns
Propellant mass	14.0	kg
Specific impulse, I_{sp}	≥ 180	s
Combustion pressure	20	bar
Propellant tank pressure	≤ 40	bar
Pressurant tank pressure	300	bar

Due to production constraints of the airframe, the entire propulsion system must be no more than 3.0 m in length and 198 mm in diameter. The thrust requirement is deduced from the target rocket mass, and I_{sp} is deduced using flight path simulations. Large components, including the propellant tanks, injector, and combustion chamber, are SRAD, while smaller components, such as valves and fittings, are COTS.

The combustion chamber is metal 3d-printed in order to utilize regenerative cooling channels as cooling method.

The fuel tank is placed inside the oxidiser tank using two concentric tubes to reduce the overall system length. See Section 6 for more information. It will be referred to as the coaxial or propellant tank.

The system is filled while the rocket is vertical on the launch rail. Two hatches for filling are located on either end of the coaxial tank. The top hatch is for filling the pressurant COPV and the separation COPV for recovery. The lower hatch fills the propellant and is accessible from ground level. Both hatches have a filling assembly with quick disconnects and manual ball valves.



Figure 4: Render of aft CAD model

5 Thrust chamber

5.1 Combustion chamber

The primary function of the combustion chamber is to provide thrust to Bifrost. The combustion chamber has a converging-diverging design and consists of an impinging injector inside the bulkhead and built-in regenerative cooling channels along the chamber walls. The combustion chamber, injector, and bulkhead are assembled using bolted connections. Thrust is produced by combustiong the Nitrous Oxide and Ethanol. The thrust is then transferred to the airframe via a load ring fastened to the aft airframe (namely the upper boattail).



Figure 5: Combustion chamber during hot-fire testing

The combustion chamber is 3D-printed in Inconel 625 by Fieldmade AS, using Selective Laser Melting (SLM) technology. This was one of two materials available from our suppliers, the other being 316L stainless steel which was less suitable for our needs. Some post-processing of the chamber after printing was necessary.

The production method constrains the chamber to a 295 mm cube. The internal diameter of the airframe limits the outer diameter to 198 mm. A maximum outer diameter of 196 mm was chosen for the chamber and the bulkhead to allow for some clearance when assembling it into the airframe. The inner chamber diameter is designed to be as large as possible while accommodating the combustion chamber walls themselves, seals, cooling channels, bolts, and passing fuel tube, in addition to its purpose of housing the injector plate, the fuel line, and mating with the sealing surface of the chamber. The final inner diameter is 130 mm.

5.1.1 Theoretical performance using NASA CEA

Propulse has developed a Python extension of NASA's chemical equilibrium with applications (CEA) program to calculate the optimal performance of the propellants chosen. The simulations used a finite area chamber, contraction ratio $A_c/A_t = 7$, and an OF range 3 to 4.

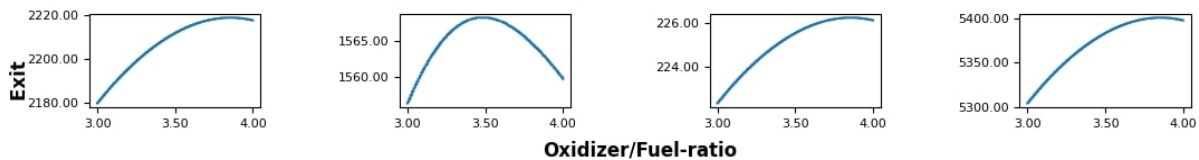


Figure 6: Performance values shown with varying OF-values ranging from 3-4.

The performance result of CEA containing the highest C^* value is shown in Table 5. From the simulation, a thrust of 5.38 kN is theoretically possible. The calculated requirement to obtain an off-rail velocity of 30 m/s, the minimum requirement for EuRoC, is 4.5 kN. Thus, a good buffer is provided. Furthermore, other values obtained from the output file are shown in the appendix Appendix K.

Table 5: Identified OF and calculated performance values for maximum C*.

Parameter	Value	Unit
C*	1568.1	m/s
O/F	3.441	—
Exhaust velocity	2209.3	m/s
Specific impulse	225.3	s
Thrust	5377.1	N

5.1.2 Inner chamber and nozzle

The dimensions of the chamber walls and nozzle diameter were calculated after the physical limitations were established. Figure 7 shows a cross section view of the combustion chamber, of which the parameters are described in table 6. The nozzle converges with a 45° angle, as that was the maximum printable overhang without using supports. Both inside and outside wall thickness of the chamber was decided to be 2 mm thick, see Appendix K.

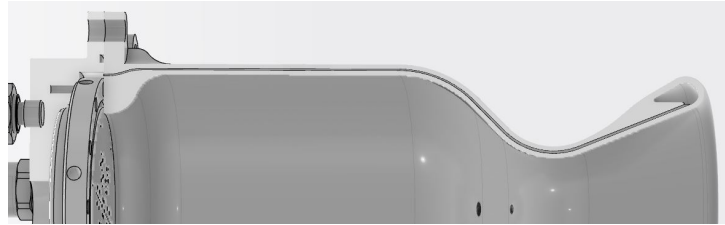


Figure 7: Profile of the combustion chamber walls and cooling channels.

Table 6: Combustion chamber main parameters.

Parameter	Dimension	Unit
Total length	295	mm
L*	1256	mm
Chamber length	220.25	mm
Chamber diameter	129.97	mm
Throat diameter	50.06	mm
Exit diameter	97.75	mm
Convergence angle (max)	45	deg
Convergence radius	49.57	mm
Divergence angle	21.7	deg

5.1.3 Cooling channels

The cooling channel design is optimized for maximum cooling effect and while keeping pressure loss at a minimum. To withstand thermal stresses during burn, the combustion chamber features a set of 70 rectangular regenerative cooling channels running along the chamber's walls, 4 mm² each. Cooling channel parameters are shown in table 7. Fuel is fed into the cooling channels through a ½" inlet connection and absorbs heat along the channel walls before being injected into the chamber. A clear view of the cooling channel outlets are shown in Figure 10. A steady state RPA thermal analysis showed regenerative cool-

ing was necessary to avoid melting: the throat could reach almost 2000°C. This cooling solution brought that down to $\sim 500^\circ\text{C}$. Details can be found in the propulsion design appendix.

Table 7: Cooling channel dimensions for chamber, throat and nozzle.

Location	Channel depth	Channel width	Unit
Chamber	0.95	4.21	mm
Throat	1.47	2.72	mm
Nozzle	1.30	3.08	mm

5.2 Injector

The primary purpose of the injector is to deliver a sufficient mass flow with a sensible pressure drop while also atomising/mixing the liquid propellants adequately. Bifrost's injector is of the like-like impinging type and is shown in figure 8. This has proven to work well during tests. The injector has $36 \times \phi 1.00$ mm orifices for fuel, and $30 \times \phi 1.90$ mm for oxidizer. The injector plate was produced in aluminum 6082-T6 using 5-axis CNC milling.

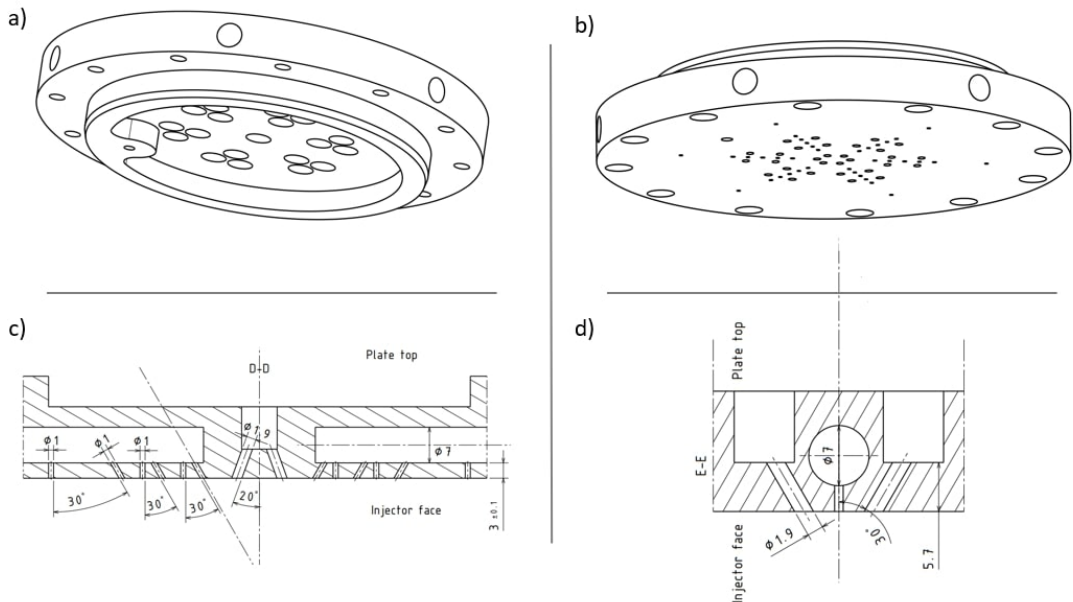


Figure 8: Machine drawing excerpt of the injector plate. a) isometric view of the injector top plate. b) injector face. c) axial view hole dimensions and angles. d) radial view of hole dimensions and angles (oxidizer).

Table 8 shows the injector parameters. The most important parameter to consider here is the injector pressure drop. Although Huzel and Huang [3, p.128] recommend 15-20% of the stagnation chamber pressure (20 bar) as injector ΔP , we choose to go as far as 78% to avoid potential chugging effects. Issues such as blowouts may occur in the transient stages of ignition, but tests prove otherwise. The feed system also manages the pressure requirements.

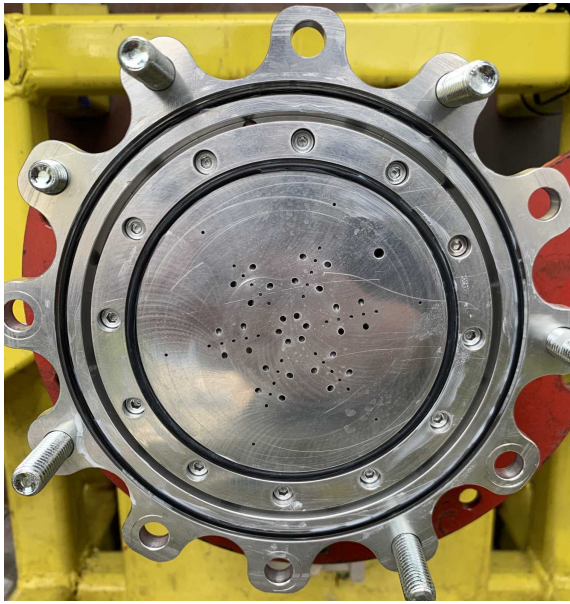


Figure 9: Injector plate mounted to bulkhead.

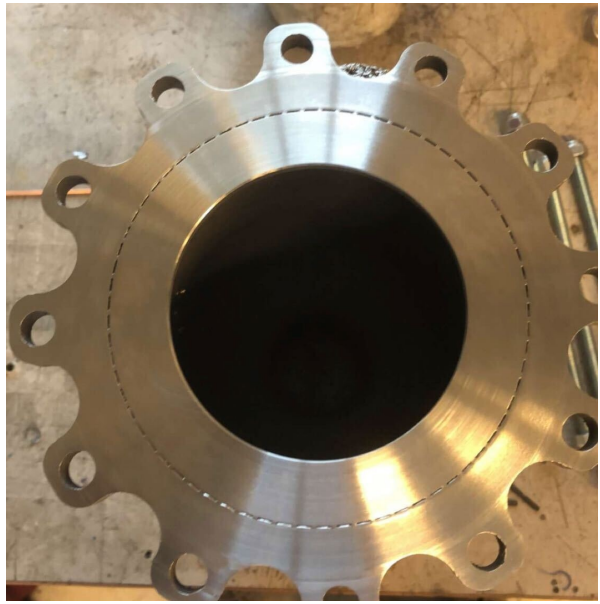


Figure 10: Mating surface of the combustion chamber, showing the circle of cooling channels.

Table 8: Injector parameters for oxidizer and fuel. Tank pressure is 40 barg and combustion chamber (nominal) pressure is 20 barg.

Parameter	Fuel	Oxidizer	Unit
Mass flow	0.575	1.973	kg/s
Orifice diameter	1.00	1.90	mm
Orifice amount	36	30	-
Orifice angle	30	30 and 20	deg
Injector C_d estimate	0.72	0.60	-
Injector ΔP (% of chamber pressure)	9.6 (48%)	15.5 (77.5%)	bar
Orifice exit velocity (axial)	20.9	20.9 and 22.7	m/s
Feed ΔP	10.4	4.5	bar
l/d	3.0	3.0	-

5.3 Bulkhead

The bulkhead has the job of containing, sealing, feeding the injector, and mounting and sealing to the combustion chamber. The bulkhead, therefore, contains a large set of seals to separate and contain the oxidizer, fuel, and combustion pressures, as seen in Figure 9 and Figure 11.



Figure 11: Bulkhead with O-rings.

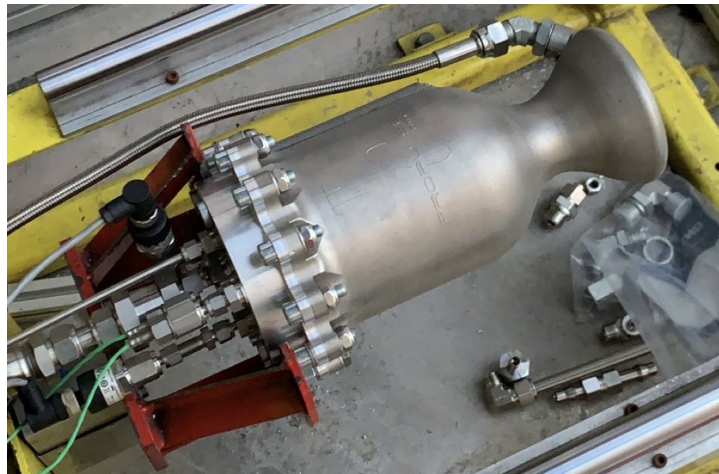


Figure 12: Assembled chamber mounted to test bench.

The bulkhead has pressure- and temperature sensors for data collection and automatic abort systems. The oxidiser inlet is placed on the top center of the bulkhead. The bulkhead is machined from a single piece of aluminum 6082-T6 using a CNC mill.

5.4 Sealing methods

The combustion chamber utilizes several Ethylene-propylene-diene-monomer (EPDM) O-rings placed in machined grooves in the bulkhead and injector. For clamping the seals between the injector and bulkhead and between bulkhead and chamber, 12x M5 bolts of 12.9-grade strength have been used. EPDM material is used for sealing as it is considered non-reactive with ethanol and nitrous oxide.

5.5 Ignition system

The ignition system is designed to ignite the combustion chamber's atomised fuel/oxidiser mixture. The igniter features a small COTS D9-P rocket motor designed for hobby rockets, mounted to a rod placed inside the combustion chamber. It is expelled automatically after ignition by the thrust produced by combustion. See appendix K for more details on startup sequence.



Figure 13: Igniter mount with shield

6 Feed system

6.1 System function and system overview

The primary function of the feed system is to provide propellants to the rocket engine during powered flight. The feed system supplies fuel and oxidiser to the engine through pipes and valves in a controlled manner, ensuring steady combustion and sufficient engine performance. Furthermore, the system must withstand the experienced combustion pressure and temperature and operate safely.

The feed system includes coaxial propellant tanks, valves, sensors, and pipelines to store, transfer, and regulate the flow of propellants to the combustion chamber. It comprises a composite over-wrapped pressure vessel, a pressurising module, a coaxial propellant tank, and a pre-engine module. This structure is illustrated with a piping and instrumentation diagram (Section 6.3).

The COPV provides gaseous nitrogen at 300 bars to the pressure regulator, which regulates the pressure to 40 bars. The nitrogen then pressurizes both the fuel and oxidiser to 40 bars. From the bottom of the coaxial tank, the fuel flows to the bottom of the combustion chamber through the regenerative cooling channels before reaching the injector. At the same time, the oxidiser is supplied directly to the injector from the oxidiser tank.

The system is also constructed to allow for refueling and propellant dumping after assembly, simplifying launch preparations and enabling rapid turnaround in case of a launch abort. Ground equipment fills the fuel, oxidiser, and nitrogen, allowing quick launch readiness. This feature offers greater flexibility and efficiency in launch operations, reducing time and resources between launch opportunities.

The oxidiser tank has a pressure control feature that uses a mechanical relief valve set at 20 bars to maintain a temperature of around -15°C during filling. This helps to maximise liquid volume and minimise the amount of gaseous oxidiser. This feature is turned off before pressurization using a servo-controlled ball valve.

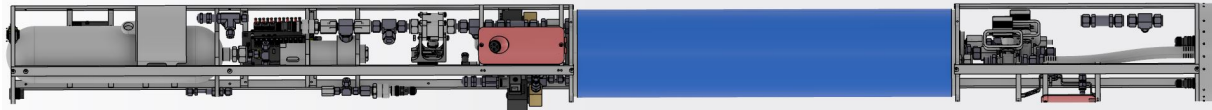


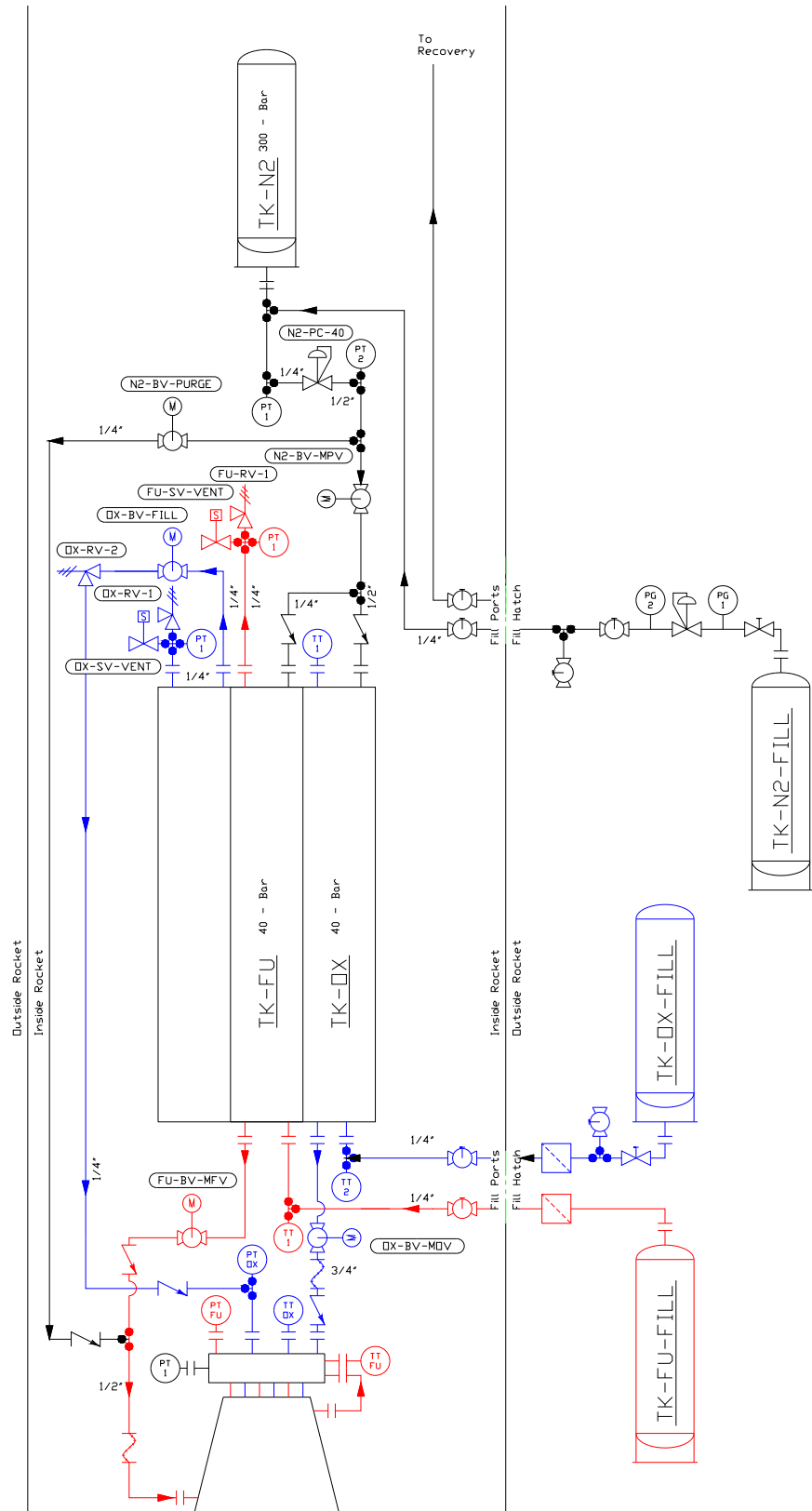
Figure 14: CAD of feed system.

6.2 Safety Features

The feed system is designed to be safe to filled manually by hand. This is achieved by utilizing low fill pressures on SRAD coaxial tank system. Maximum fill pressure during hand filling of propellants is 13 bars, which gives an factor of safety of 6 in therms of pressure. For the N2 loading, all components in the system are COTS. This, combined with strict procedures and high standard of personnel practice with over 50 cold- and hotfire test runs, gives the team the certainty that the filling operation can happen in a safe manner.

Additionally, the fuel and oxidiser tanks have both a pressure relief valve and a solenoid valve on top to relieve pressure in case of over-pressurization and depressurize the tanks in case of an abort or loss of power. The COPV can be depressurized manually by opening its fill port or remote by depleting N2 through the propellant tanks. In an abort where the tanks need to be emptied, the fuel can be drained through its fill port while the oxidiser can boil off through the solenoid above the valve on top of the tank. There is also a purge system to purge all fuel out of the cooling channels after burning with gaseous nitrogen to avoid fuel boiling inside the cooling channels.

6.3 P&ID



6.4 Propellant storage



Figure 15: CAD of the coaxial propellant tank.

Both propellants are stored in a custom-made coaxial tank where the fuel tank resides within the oxidiser tank. This design was chosen as it shortens the rocket length by up to one meter and makes routing tubing in the pre-engine module significantly easier. The coaxial vessel is designed to withstand the pressure and external forces experienced during testing and nominal launch, as well as those caused by its operating pressure of 40 bars. It is designed and tested according to EuRoC DTEG and R&R. This includes

- Safety factor of no less than 2
- Hydrostatic pressure test at 1.5x MAWP
- Relief valve set no higher than 1.5x MAWP

The outer diameter is set to 178 mm to leave 10 mm clearance to the airframe on either side of the tank. This allows for cables and auxiliary pipes to pass. The fuel tank is 10 mm longer than the oxidiser tank on each end to aid welding. The components are manufactured to the specified dimension and then welded by a partner company. The outer surface underwent an anodizing process to decorate the surface with a metallic blue color.

Table 9: Coaxial tank design values.

Parameter	Oxidiser section	Fuel section
Volume	12.3 L	4.2 L
Cylinder length	750 mm	770 mm
Nominal cylinder thickness	4 mm	3 mm
Cylinder diameter	Ø178 mm	Ø90 mm
Bulkhead thickness	8 mm	8 mm

6.5 Pressurising system

The pressurising system comprises the N2 COPV, a pressure regulator, a common pressurization valve, and a purge valve.

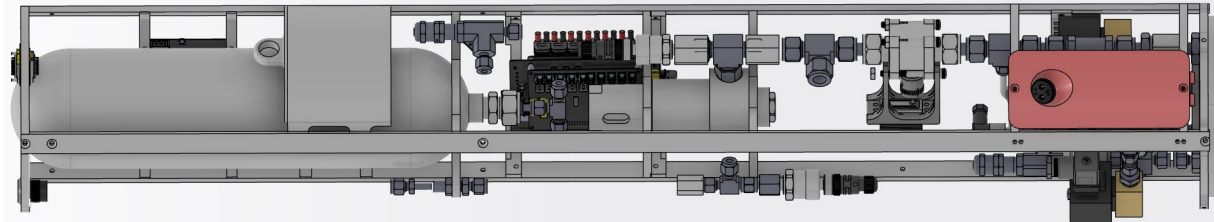


Figure 16: CAD of pressurization module. Not all tubing is shown due to visibility.

1/4" tubes are used for the 300 bar section but increase to 1/2" after the regulator. The 1/2" tube goes into the oxidiser tank and breaks off in a tee to have 1/4" to the fuel tank. There are separate one-way valves before the tank inlets to ensure no back-flow or mixing of propellants upstream of the tank.

The N2 COPV will heat up during filling and cool down during the burn. To ensure the tank temperature does not rise above 60 C, which is the test pressure, the tank is filled to 300 bars for several minutes. The minimum tank size is calculated using the isothermal expansion of an ideal gas. This yields a lower volume than using adiabatic expansion. Nonetheless, the volume is large enough to provide sufficient gas during the start of the burn, which in turn helps produce sufficient off-rail velocity.

Table 10: Details on COTS pressurant COPV.

Liner material	Wrapping material	MAWP	Water volume	OD	Length	Mass
6061-T6 Aluminium	Glass fibre composite	300 bar @ 15 C	3.0 L	114 mm	443 mm	1.9 kg

A single, high-performance pressure regulator from Tescom is used. Using two separate regulators would allow for more flow control in the system. Only one regulator is used due to the high mass of the regulator. The regulator is placed close to the center of gravity for the same reasons.

Table 11: Pressure regulator details for Tescom 44-1365-9082-002.

Body material	Inlet pressure	Outlet pressure	Port	Orifice	Mass
316 SS	310 bar	0-69 bar	1/2" F-BSPP	3/8" C _v 2.0	2.8 kg

6.6 Flow control

To control flow through and to the various parts of the propulsion system, the feed system employs a variety of valves. Manual ball valves are used for filling to give more control to the ones filling the tanks. On top of both the fuel and oxidiser tanks, there are open solenoid valves to depressurize the tanks. The tanks have a relief valve to ensure the tanks aren't over-pressurized. In addition, the oxidiser tank has a servo-controlled ball valve followed by a relief valve to lower the filling pressure. A servo-controlled ball valve for purging fuel from the cooling channels is connected to the pressurising line. The main oxidiser and fuel valves are servo-controlled ball valves. All servo and solenoid valves are controlled by propulsion avionics (Section 10.3.3). A full overview of the valves employed in the system can be found below:

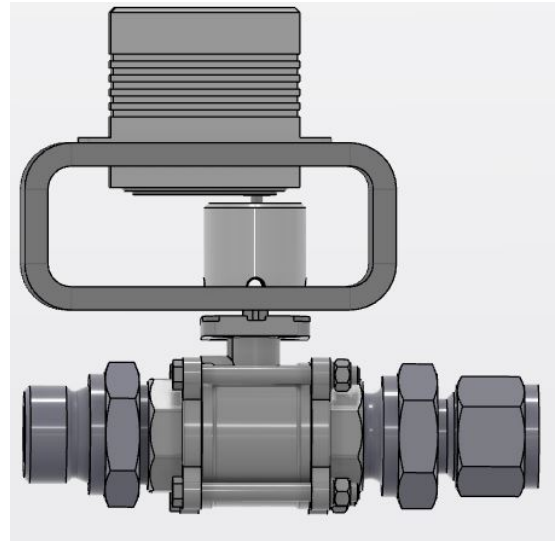


Figure 17: CAD of main valve assembly including V-port ball valve, servo motor, and actuator mounting bracket.

Table 12: Overview of all valves in the feed system.

Placement	Type	Actuator	Orifice size	Normal state
Fuel fill	Full-bore ball	Manual	1/4"	N/A
Ox fill				
N2 fill				
Rec. fill				
Fuel vent	Direct-acting solenoid	Solenoid	1 mm	Open
Ox vent				
Fuel pres. relief	Relief valve	Spring-return	Variable	Closed
Ox. pres. relief				
Ox fill vent	Full-bore ball	Servo	1/4"	N/A
	Relief valve	Spring-return	Variable	Closed
pressurising	Full-bore ball	Servo	1/2"	N/A
Fuel purge	Full-bore ball	Servo	1/4"	N/A
MOV	V-port ball	Servo	1/2" 90 deg	N/A
MFV			1/2" 30 deg	

7 Outer structure

7.1 System function and system overview

The main function is to ensure stability and retain the structural integrity of the rocket's airframe. Therefore, a good stability margin must be ensured during the entire flight. Stable is defined as maintaining a static margin of at least 1.5 to 2 body calibers, regardless of center of gravity (CG) movement due to depleting consumables and shifting center of pressure (CP) location due to wave drag.

The outer structure of the rocket, as shown in figure 18, is divided into 7 different parts. These parts do not include the coupler between the aft airframe and the forward airframe or the coupler between the forward airframe and the nosecone, as these are designed by inner-structure and recovery disciplines, respectively. All parts closely align with aerodynamic standards to ensure flight stability. Furthermore, it must also be verified that the outer structure can withstand the forces and operating stresses acting on it.

The tasks mentioned above must be accomplished, and an accurate trajectory simulation must be performed to fulfill the goal of reaching apogee.

7.2 Nose Tip

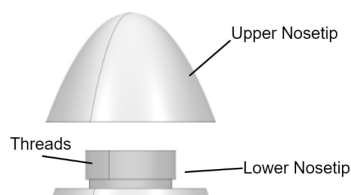


Figure 19: Nosetip overview

Function

The aerodynamic properties of a rocket are influenced by the shape and design of its nose tip, which serves as the final point of the load-bearing structure.

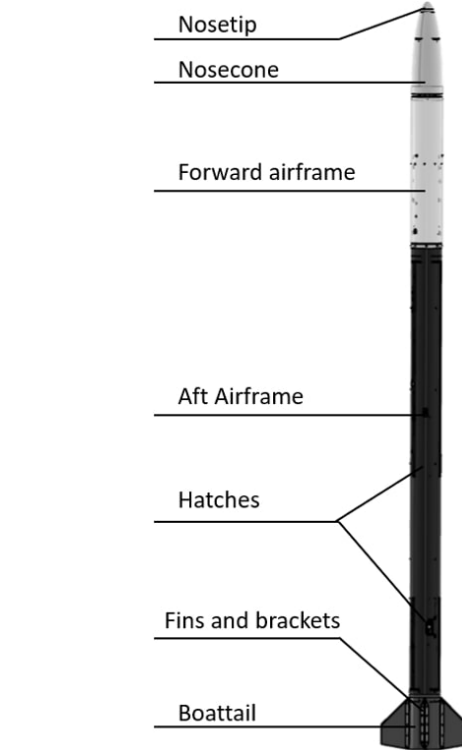


Figure 18: Full outer overview

Design

The design of the nose tip follows an elliptical shape. Our previous flight-proven launches employ a similar design, but we must scale it up to fit Bifrost's larger size. This shape is the most efficient form for the rocket's speeds. There is no connection between the nose tip and the payload, so the nose tip divides into 2 parts. The lower part will be glued inside the airframe, and the upper part will be screwed in the lower part of the nose tip as the part is threaded.

Manufacturing decisions

It will be made with CNC-turning at Byåsen VGS. All aluminium parts in the outer structure are made by 6082-T6 aluminium.

7.3 Nosecone

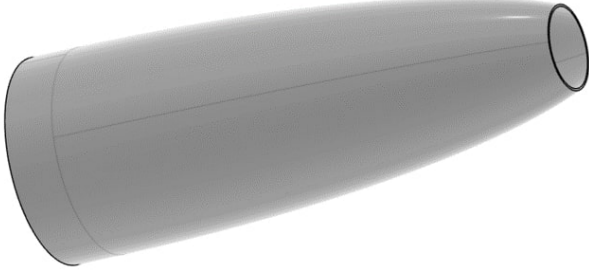


Figure 20: Nosecone model

Function

The nose cone of a rocket plays a crucial role in reducing drag and optimizing its aerodynamic performance. To achieve this, it must be designed with the utmost attention to its shape and structure, ensuring it can withstand the stresses of takeoff, flight, and landing while retaining its integrity. In addition, the material used in constructing the nose cone must be radio transparent, as it contains vital components such as the payload and GPS. The upper and lower airframe are also designed to be

load-bearing, contributing to the overall structural integrity of the rocket.

Design

The rocket's nosecone will be designed in an elliptical shape, as Aditya Rajan Iyer and Anjali Pant recommended in their 2020 review of nose cone designs for different flight regimes. According to their findings, for subsonic flight (below Mach 0.8), the nose pressure drag is essentially zero for all shapes, and the primary factor affecting drag is friction, which is determined by the wetted area, surface smoothness, and shape discontinuities. A short, blunt, smooth, and elliptical shape is typically the most optimal for subsonic rockets. Since the Bifrost rocket has a maximum Mach number of 0.72, an elliptical nosecone is preferred. The nosecone and tip will be the only airframe parts that taper to fit the elliptical shape when the rocket is fully assembled. The nosecone will be 600 mm. The upper airframe will be constructed using Zentron 758 S-2 glass fibers and UF3369 epoxy to ensure radio transparency.

Manufacturing decisions

In composite airframe production, we use filament winding to wrap pre-impregnated fibers around an elliptical mandrel, forming the structure after curing. Post-processing like polishing and painting ensures the desired surface finish. Winding Technology AS is our partner for production and finishing. The mandrel shape matches the exterior's elliptical form, narrowing to fit densely packed filaments at the nosecone. CNC machining will create this custom mandrel, matching the 198mm airframe diameter at the end. An additional epoxy layer precedes sanding for a smooth nosecone. Wall thickness variances with the airframe taper is accounted for in design and simulations.

7.4 Forward Airframe

Function

The forward airframe is a critical component of the rocket, housing the chute bay, recovery systems, and avionics. The forward airframe is located directly under the nose cone and must be designed to withstand the forces and stresses generated by the rest of the rocket during flight.

One of the key design considerations for the forward airframe is the selection of a radiotransparent material. This will ensure that the avionics systems can communicate with the ground station throughout the flight and provide real-time telemetry data.

Design

The forward rocket airframe prioritizes simplicity and efficiency. It will adopt a cylindrical design with a 198mm inner diameter, utilizing an available mandrel to minimize complexity and costs, as shown in Figure 4.3.1. This design also guarantees a snug fit for internal components. The airframe's length is set at 950mm. To support ground-to-avionics communication, we'll use radio-transparent glass fiber material, ensuring signal transmission without interference while preserving airframe integrity and durability.

Manufacturing decisions

The production method for the composite airframe is filament winding. In this process, pre-impregnated fibers are wound at different orientations around a mandrel. After curing, the composite structure is complete. Post-processing, such as polishing and painting, is required to achieve the desired finish. The airframe will be produced at Windinc Technology AS through a sponsored partnership.

7.5 Aft Airframe

Function

The aft airframe is an essential component of the rocket's design, serving as a protective housing for the self-produced liquid engine motor and providing access to the inner structure and fill ports through hatches. It has to be structurally sound to ensure that it can withstand the stresses and loads of launch and flight.

Design

The aft airframe has been designed to house the self-produced liquid engine motor, provide access to the inner structure, and fill ports through two conveniently located hatches. Unlike the upper and forward airframes, radio transparency is not required for the lower airframe, allowing us to utilize the highly durable and lightweight carbon fiber material. Using a pre-existing mandrel from Winding Technology AS allows us to reduce costs. This limits the inner diameter of the rocket to 198mm. The length of the aft airframe is 2511mm.

The aft airframe serves as the housing for the self-produced liquid engine motor and provides access to the inner structure and fill ports through two conveniently located hatches. Unlike the upper and forward airframes, radio transparency is unnecessary for the aft airframe, allowing durable and lightweight carbon fiber material to be used. Utilizing the same mandrell as the forward airframe gives a diameter of 198mm and a length of 2511mm.

Manufacturing decisions

The aft airframe and the boat tail have been produced with a mandrel from Winding Technology AS. The same process as for the nosecone was used for manufacturing. The Hatches were machined using a drill and an angle grinder before the edges were sanded to avoid delamination.

7.6 Launch lugs

Function

To secure the rocket to the launch rail during launch. Lend support to the rocket until it reaches adequate speed for a stable and safe launch.

Design

The design is based on the regular launch lug design used during EuRoC. Three lugs will be used - where the top lug is mainly for extra support while waiting to launch - and the middle lug is slightly above the Cg. To have as much contact time with the launch rail as possible, the bottom two lugs will be placed as low on the rocket as possible. Thereby allowing for a high off-rail velocity and a safer flight. The lugs are placed close to the Cg as to reduce forces acting on the lugs.

Manufacturing decisions

The launch lugs are SLS-printed with continuous carbon fibre. It is imperative to the stability of the flight that the launch lugs are robust enough to withstand the forces during launch.

7.7 Hatches

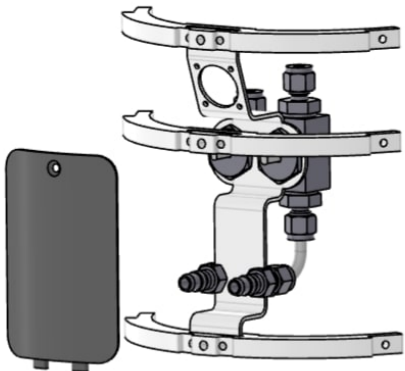


Figure 21: Lower Hatch

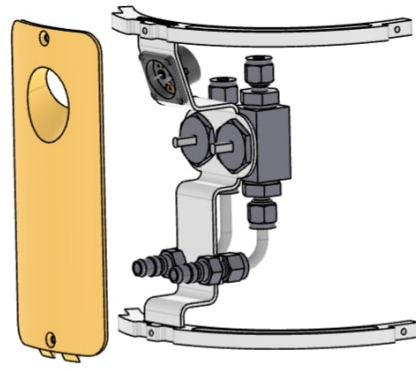


Figure 22: Upper Hatch

Function

Feed systems require direct access to the internal fuel systems for filling tanks, leakage concerns, and the ability to iterate the motor and check sensors while the rocket is assembled. There is also a need for recovery systems and a place to have the umbilical cord that doesn't damage the integrity of the airframe. Therefore, some access points have to be created. This will be integrated in the form of two hatches.

Design

There are two different hatches that each have their unique design. The first hatch is the recovery hatch close to an inner structure rail. It is smaller than the other hatch since it is the only place for recovery readiness and the umbilical cord. It is screwed in place in fasteners connected to the hatch's inner structure at the top and bottom. To avoid vibration, it is pushed in the fastener. The size is 6.57 cm x 17.5 cm. The second hatch is larger and between two inner structure rails. It will be screwed into fasteners placed on the inner structure rails. The lower pad of the hatch holds the fin in place to the outer structure, and the fasteners in the inner structure defend the bracket from all vibration. The size is 6 cm x 11 cm, but it is possible to lower it if necessary.

Manufacturing decisions

The hatches have been made by 3D printing in Pa6-cf nylon, and the fastener for the hatch has been laser cut. The hole corners for the hatches were drilled out at Winding Technology AS, and the rest was cut with an angle grinder.

7.8 Fins and fin brackets

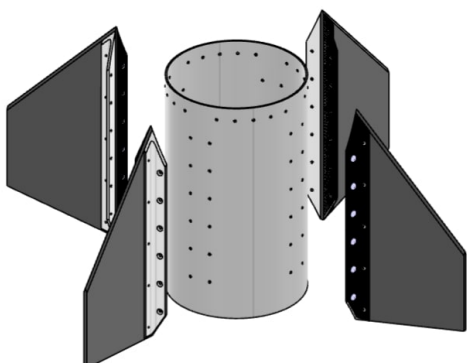


Figure 23: Exploded view boat tail - with brackets and fins

Function

The rocket fins are multi-functional, ensuring stability by shifting the center of pressure downward and preventing roll. They require precision in design and manufacturing for tight alignment, aerodynamic efficiency, and durability during flight. Simultaneously, brackets secure the fins to the airframe, withstanding launch forces.

Design

The design of the fins has been changed compared to previous projects for enhanced performance. Specifically, the rear fin angle is extended to 80 degrees, shifting the center of pressure (CP) further backward. This adjustment improves stability without exposing the fins to potential damage upon landing. The fins measure 340 mm in length and 180 mm in height, providing a stable margin. Their length matches the boat tail to simplify engine mounting. The front of each fin retains a sharp angle to uphold aerodynamic efficiency. Additionally, the brackets were meticulously crafted for aerodynamic optimization, featuring countersunk bolts and angled edges to minimize drag. Each fin is fastened with five bolts to the bracket, while four bolts secure the brackets to the aft airframe.

Manufacturing decisions

Manufacturing the fins in-house involves the prepreg layup method, which includes layering carbon fiber sheets with resin impregnation. Subsequently, every layer undergoes heat treatment. The fin shape is then cut out from the carbon fiber plate using water cutting. In contrast, the brackets have been machined from aluminum.

7.9 Boat Tail

The boat tail serves a dual purpose in the rocket design. Firstly, it shields the combustion chamber from the airflow, thus reducing drag, improving efficiency, and shielding it from the impact of landing. Secondly, it provides a secure attachment point for the fins, essential for aerodynamic stability and control during flight.

Function

The boat tail will be tube-shaped with a length of 340mm longer than the burn chamber, reducing the chance of the burn chamber being damaged during landing.

Design

The boat tail uses the same winding process and carbon fiber material as the aft airframe, forward airframe, and nosecone. This ensures uniformity and consistency throughout the rocket's structure, providing the strength and durability to withstand the extreme forces experienced during launch and flight. The boat tail will be fastened to the upper boat tail - and thereby the rest of the rocket - with screws. As seen in Figure 23, screw holes are added for fastening the boat tail to the upper boat tail.

7.10 Composite validation

Flight data and theoretical calculations have been used to simulate the working conditions of the various composite components. Said values can be found in Appendix A, B, and C. The simulations are conducted in ANSYS workbench. The safety factor for each component is listed in Table. As the moment forces on the boat tail are negligible, there is no analysis of these forces.

Table 13: Parts, their incident forces, and the resulting safety factor after composite analysis.

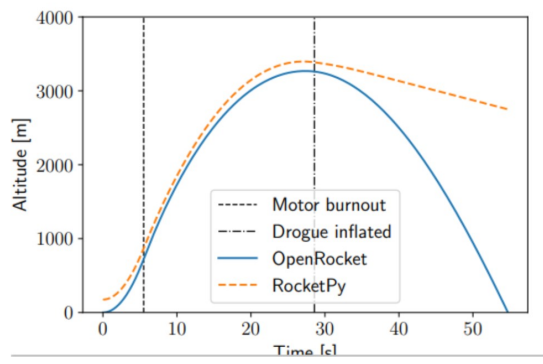
Part	Incident forces	Factor of safety
Nose cone	Forces from nose tip, max pressure nose cone	8.8
Forward	Pressure forces from nose tip and nose cone	20.56
Aft	Pressure forces from nose tip and nosecone, Shear and Moment forces, Acceleration forces	1.91
Boat tail	Kinetic energy of the rocket at touchdown divided by a time of 0.1 seconds	3.04
Fins	Max force fins, max pressure fins	4.93

7.11 Flight validation

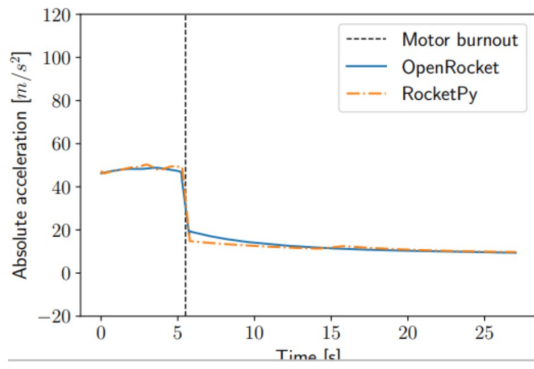
Flight statistics have been gathered primarily from OpenRocket, rocketpy and CFD analysis. For simplicity, the most important results are posted below. More in-depth analysis and CFD can be found in the appendix. The analytical results yield an off-rail velocity of 30.8 m/s - 0.8 m/s above the required speed. In addition, the analysis has achieved a stability margin of 2.32-4.17 calibers. Thereby indicating a stable and safe launch for Bifrost. Further calculations and results can be found in Appendix N.

Table 14: Important flight values.

Simulation conditions	Value	Results	Value
Launch elevation [moh]	160	Apogee [m] (AGL)	3251
Atmospheric model With an initial temperature [$^{\circ}$ C] and initial pressure [Pa]	ISA 20 99450	Max velocity [m/s] (Mach)	268.7 (0.792)
Avg. windspeed [m/s]	3.23	Max acceleration [m/s 2]	76.649
Standard deviation [m/s]	0.15	Off Rail velocity [m/s]	30.744
Rail angle [$^{\circ}$]	6	Time to apogee [s]	27
Rail length [m]	12	Impact velocity [m/s]	7
Stability margin	3.5-4		



(a) Figure 10: Flight path of the rocket



(b) Figure 11: Acceleration during flight. Stapled line is time at motor burnout

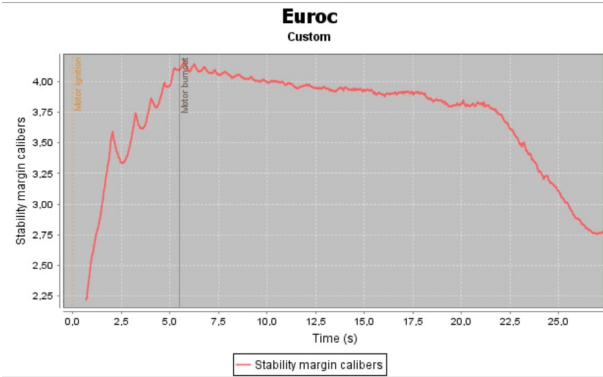


Figure 25: Stability of the rocket from off rail to separation.

8 Inner structure

8.1 System function and system overview

The main function of the inner structures is to provide a sturdy framework for mounting components within the rocket. The outer structure is the load bearing of the engine thrust. Inner structure needs to withstand the forces of its own weight, vibrations when accelerating, as well as deceleration when recovery parachutes are released and impact from landing. Figure 26 provides an overview of the inner structure.

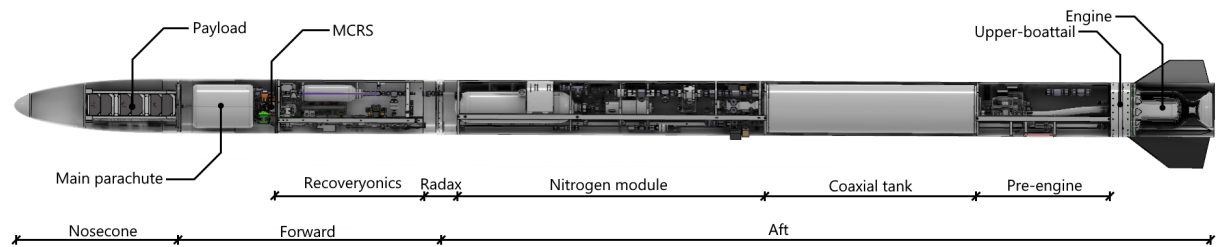


Figure 26: Overview of related inner structure

Constraints on the designs are mainly the production of the parts. Easy and cost-effective production is a priority in our design, whilst having lightweight parts, and an easy assembly process. Production methods are also a constraint, where access to advanced production methods is limited, so only a small selection of parts are, for example, made in a CNC-machines.

8.2 Payload module

The payload module's primary function is to safely and practically contain the payload. Dimension of the payload is 100x100x330mm, and it is a satellite made by Orbit NTNU. Reference Figure 27, the frame of the satellite is designed to take loads through the corners of the satellite frame. The module only has contact with the corner legs, to not come in the way of the satellite side panels. Lastly, the payload module is located in the nosecone.

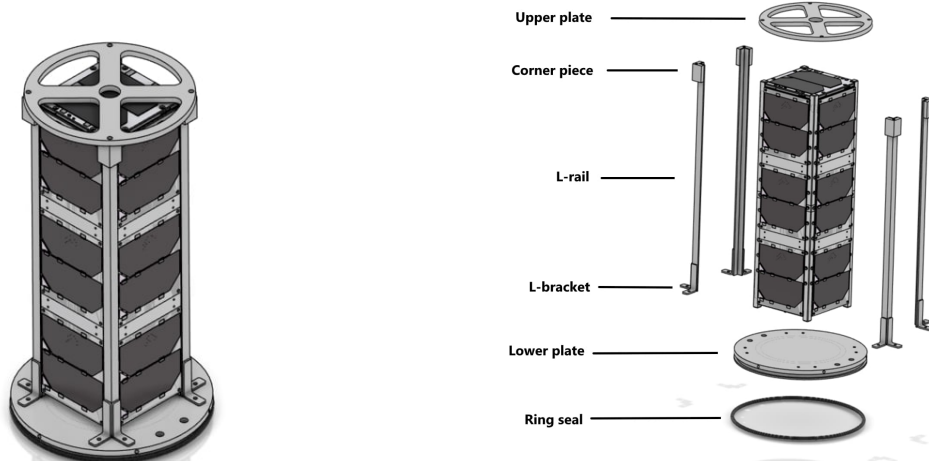


Figure 27: Assembled payload module

Figure 28: Exploded view of payload module

The payload module consists of six central components and twelve lesser components. See Figure 28 for an overview. M4 bolts and nuts are also used. One only needs to unscrew four bolts at the upper plate to

insert the satellite.

The module itself, with the satellite, will be assembled into the nosecone in the following steps: First, the module will be put through the recovery coupler, and the upper plate will be pressed up against the wall of the nosecone. When the upper plate is pressed against the nosecone, the lower plate will be fastened to the recovery coupler with eight M4 bolts.

8.3 Radax joint

The radax joint's main goal is to ensure secure connections between the forward- and aft parts of the rocket. The ideal material for the rocket is carbon fibre; however, it is conductive and will block radio signals from the avionics in the forward module. Glass fibre is radio-transparent; therefore, a joint is necessary to connect the rocket. The joints will be glued to the airframe, making a stiff and sturdy connection between the rocket airframe.

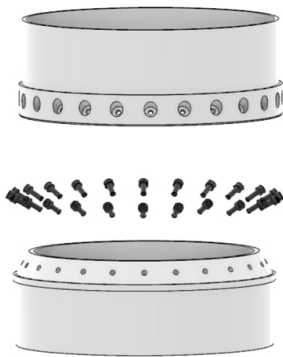


Figure 29: Exploded view of assembled radax joint

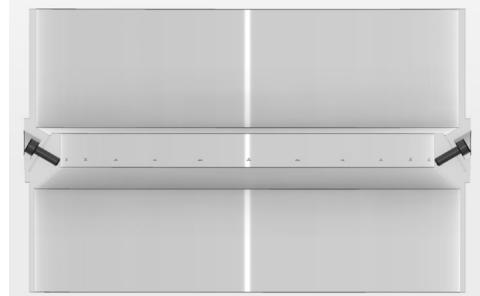


Figure 30: Section of the joints

The design consists of two cylindrical parts, the forward- and aft radax joint, one male and female counterpart, reference Figure 29 and Figure 30. The parts will connect conically, with an angle of 30 degrees. The joints will be connected with a chosen amount of M4 socket bolts, but no less than eight have been decided. Wire-threaded inserts will be inserted in the holes due to the material difference between the bolts and the joints. Steel bolts will tear aluminum threads easily. The joints will be permanently glued to their corresponding airframe, thus reducing the holes needed.

Below is a table of key results from the FEA analysis of the joints, Table 15. The results differ due to how the part is processed before the simulation. Both experience the same amount of force and generally have a similar design and mass. There were also conducted tests to see how much force the bolts and wire threaded inserts can endure, Appendix L.

Table 15: Results from FEA analysis on forward- and aft radax joint

Applied forces	Values	Result type	Forward radax result	Aft radax result
Engine	2000N	VonMises	12.1MPa	49.6MPa
Drag	400N	Displacement	0.0033mm	0.0074mm
Shear	112N	FoS	22.3	5.44
Bending moment	212Nm			

8.4 Recovery and avionics module

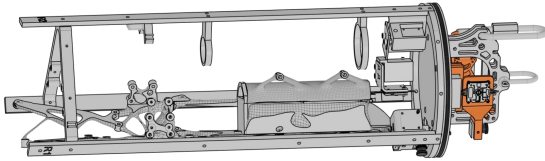


Figure 31: Bare version of the recovery and avionics module

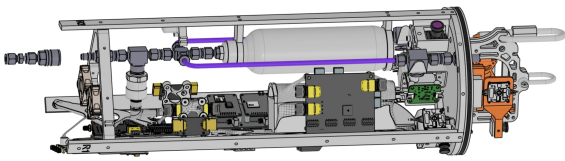


Figure 32: Recovery and avionics module with components

Function

The function of the avionics, Figure 31, and recovery, Figure 32, module is as follows:

- Fastening of the electrical components
- Fastening of the recovery system
- Easy removal of individual components
- Facilitate easy cable management
- Designed for ease of assembly
- Be modular

Design

The design follows a modular approach that enables us to assemble the components separately from the rest of the rocket. It consists of a single module ring and three rails, of which the parts are fastened to Figure 31. To minimize vibrations and reduce the risk of buckling, the module ring matches the inner diameter of the airframe, and all screw holes are countersunk to achieve a flush fit.

Moreover, the recovery and avionics module prioritizes ease of assembly and modularity. This entails designing with fewer fastening points, allowing separate assembly of the recovery and avionics systems while maintaining the inner structure's structural integrity.

This is accomplished by fastening the avionic mounting plate to two rails and the recovery system to the third rail. Unscrewing three screws makes it possible to remove the mounting plate, enabling separate work on the two systems.

Mounting plate

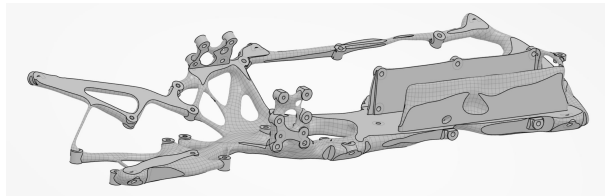


Figure 33: Mounting plate

The mounting plate, Figure 33, is designed with a V-shaped contour to match the airframe's curvature closely. It is topology-optimized, reducing the plate's volume and weight and creating additional room for improved cable management.

Component fastening



Figure 34: Heated insert



Figure 35: Vibration dampening standoff

All of the electrical components are fastened using screws. Heated inserts are used in 3D printed material for threading, Figure 34. Vibration dampers are useful on more sensitive equipment, Figure 35.

Camera mount

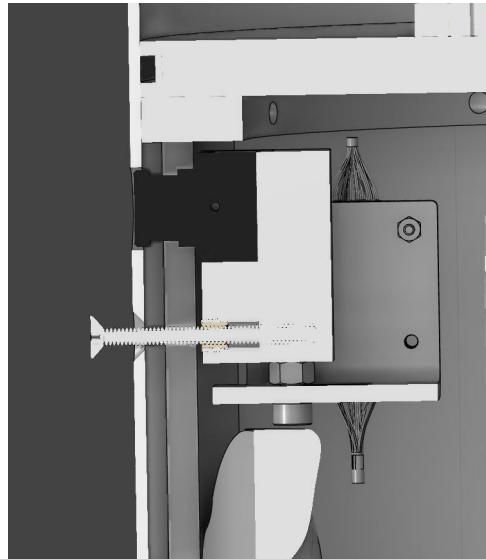
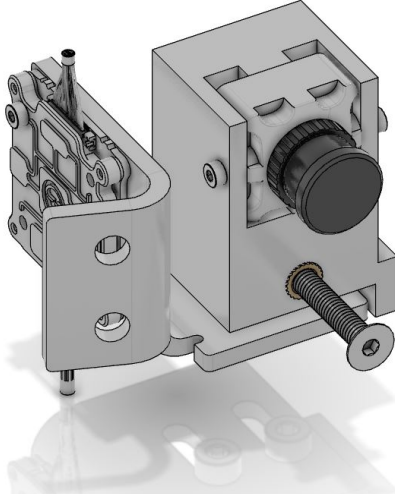


Figure 36: Run cam assembly ¹, and cross-section in recovery and Avionics module

The camera can't be extended when assembling the module into the airframe. Thus, we need to extend it afterward by turning the screw. In Figure 36, the screws are mounted in a slot that allows the camera to move forward.

Manufacturing decisions

The structure needs to be light, strong, and easy to manufacture. Therefore, laser-cut aluminum was chosen for most metal components. The mounting plate is manufactured using SLS 3D printing, eliminating the need for a support structure when printing.

The material used is PA12/PA2200 nylon, chosen for its 48 MPa tensile strength, 930 kg/m³ density, and high heat deflection temperature (175°C @ 0.45 MPa). The material also has holes built into the mounting plate, allowing heated threaded inserts of sizes M2-M4 to be installed using a soldering iron. Heated inserts are suitable for thermoplastics like PA12 nylon as the plastic melts momentarily and stiffens around the insert, resulting in a strong thread in the plastic part.

¹There are two Runcam assemblies and one Firefly assembly. Firefly camera can live stream video.

8.5 Aft end

The aft end of the rocket consists of 4 critical parts.

1. Nitrogen module
2. Coaxial tank (covered in 2.2-*Propulsion*)
3. Pre-engine module
4. Upper boat tail

Breaking the aft into modules gives flexibility to assembly. Module rings, tank mounts, regulator mounts, and rails act as the framework where module rings and tank mounts intersect the inner structure components and the airframe.

This section of the report details some decisions, architecture, calculations, and FEA on the upper boat tail and tank.

The parts are mainly water-cut; the upper boat tail is made by turning and milling. Water cutting is a cost-effective option; the boat tail has a complex geometry to reduce weight. Unoptimized parts weigh 1.7 kg, whereas the optimized mass is 1.3 kg.

To have a smooth assembly process, we decided to streamline the choice of screws—M4 for airframe to the inner structure components and M3 for avionics to engine components.

Nitrogen module

The nitrogen module, Figure 37, is the largest module in the rocket. Some critical parts include the N2 line to coaxial tanks that pressurize the push-down of fuel and oxidizer and engine components that control valves and the battery.

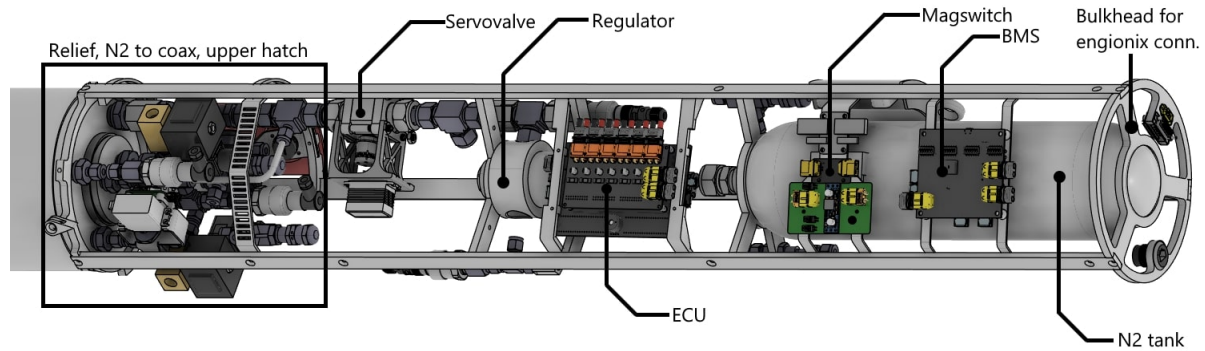


Figure 37: Overview of the nitrogen module

This module also contains an upper hatch (not visible in the picture above). It contains two valves with Swagelok 1/4" connectors to fill the nitrogen tank, the recovery COPV, and umbilical cords for charging on the launch site.

8.5.1 Pre-engine

The purpose of this module, Figure 38 is to connect the tanks to the engine and provide a filling point; there are servo valves to control flow to the engine. Due to regulations, the hatch for filling needs to be below the tank to allow gravity to empty the tanks on the launch pad if necessary.

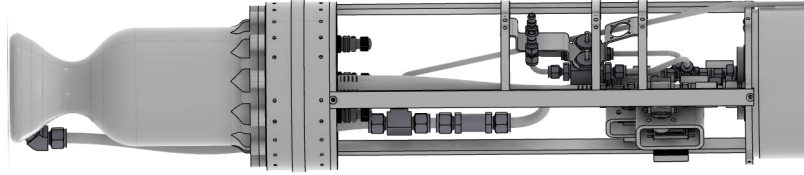


Figure 38: Pre-engine module

Upper boat tail (force transfer)

The upper boat tail intersects the engine, inner-, and outer structures. The boat tail design is critical to withstand the forces of the engine and the reactionary forces of the airframe during launch.

This FEA, Figure 39 and Table 16, is for a CNC-optimized design and represents the least mass required to withstand the forces. The mass is at 0.86kg. Due to production limitations, another design was necessary to accommodate turning and milling.

However, the analysis is still valid, as the safety factor exceeds 2.1, and the analysis converged, Appendix M. The major changes include increased wall thickness and more holes for connecting the airframe.

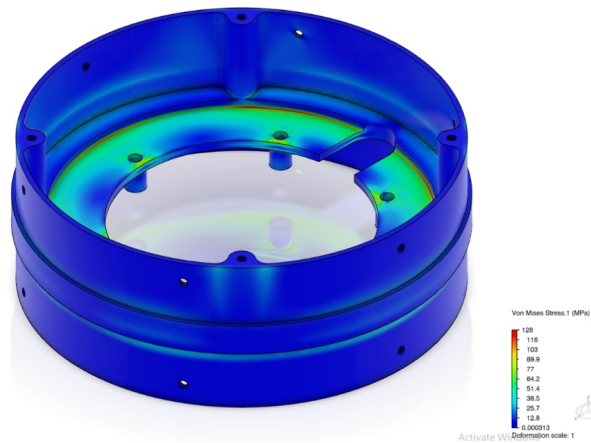


Table 16: Results FEA

Applied forces	Values	Type	Values
Engine	4500N	VonMises	128MPa
Weight, drag	7200N	Displacement	0.221
Shear	112	FoS	2.1
Bending moment	12Nm		

Figure 39: FEA analysis, VonMises(stress)

8.6 Connections to airframe

Screws are used to fasten the outer structure to the inner structure. Calculations have found M4 screws as the best solution for all connections to the airframe and inner structure Appendix M. In addition, many screws are interchangeable between different parts. This reduces the chance of confusion and miss-assembling, primarily when electronics use M3 screws.

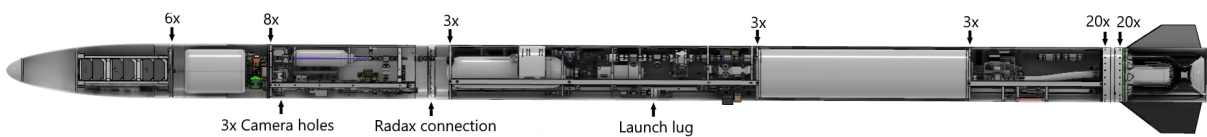


Figure 40: Each arrow marks a hole, and every arrow on the upside marks $\phi 4.2\text{mm}$ in the airframe.

Each camera has a $\phi 15\text{mm}$ hole and a $\phi 4.2\text{mm}$ hole, see paragraph 8.4 on the camera. In Figure 40 the

camera holes totals to six, two per camera. The radax is glued to the airframe, so no connections except forward- and aft-radax joints are necessary. Launch lug requires a Ø4.2mm hole.

9 Recovery

9.1 System function and overview

The recovery system is a dual-deployment parachute recovery. The system features a drogue parachute and a main parachute. The drogue parachute will be deployed at or near apogee using a pressure-based separation system (PBSS). The main parachute is deployed at 400 meters AGL using a mechanical SRAD main chute release system (MCRS). Figure 41 shows the complete recovery system.

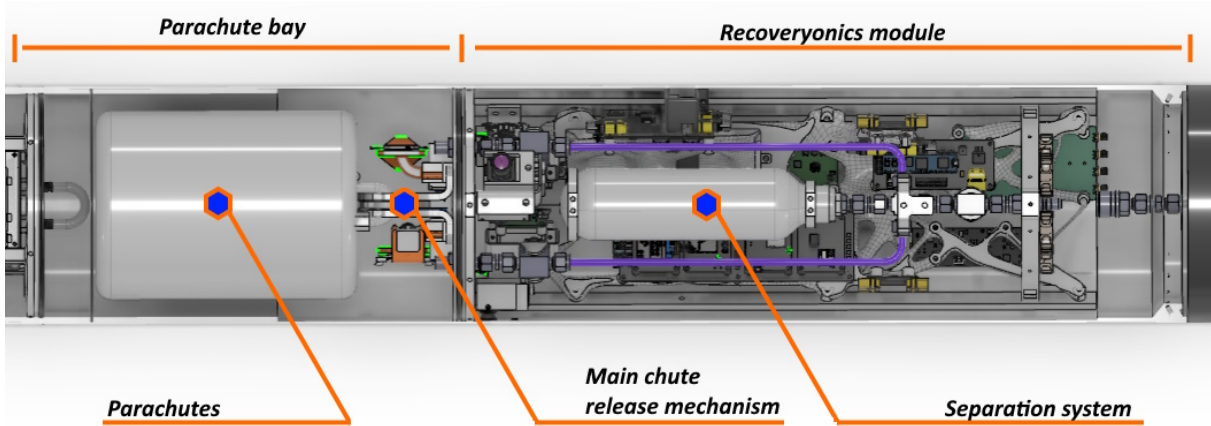


Figure 41: Recovery system overview.

9.2 Separation system

The function of the PBSS, shown in Figure 42, is to separate the nosecone from the forward airframe at apogee, thus ejecting the drogue parachute using compressed air. It consists of a pressure vessel pressurized to around 100 bar, with two valves that can be actuated by the COTS and the SRAD flight computer (FC), respectively. The pressurized gas flows through the tubing, leading into the parachute bay. Moreover, the nosecone is fastened to the forward airframe using a coupler and nylon screws, also known as shear screws. With enough pressure build-up inside the parachute bay these screws shear, separating the nose cone from the rocket.

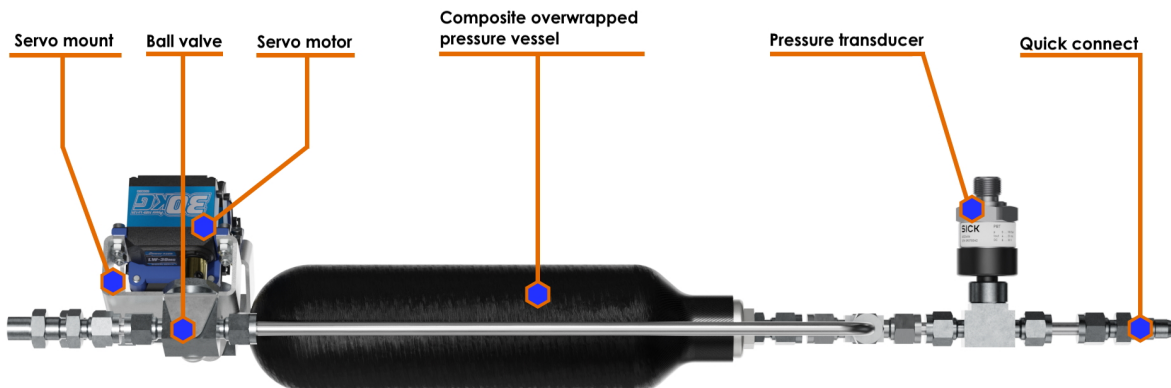


Figure 42: Separation system overview.

The system features redundant electronics where one of the valves is actuated by a servo motor that the CATS Vega FC controls. In contrast, the other valve is actuated by a servo motor controlled by the SRAD FC. For separation to occur, it is enough for only one of these valves to be actuated. However, the system is not mechanically redundant; leakage is the most likely failure mode. To mitigate this, a pressure transducer monitors the pressure in the COPV. A thorough description is given in Appendix D.

To accommodate the rules regarding the safing and arming of energetics, the COPV will be pressurized when the rocket is in the launch position. As illustrated in Figure 43, filling happens through a hatch in the airframe located closer to the ground.

Shear screws

The nylon screws function as a controlled structural weak point. The screws need to be dimensioned to break as intended during PBSS activation but also be resistant enough to withstand the forces during the ascent and handling of the rocket. During ascent, the difference in drag on the aft and forward airframes results in a shear force on the screws. However, the shear force is typically negligible compared to the pressure gradient force at apogee. Assuming an airtight recovery chamber, a pressure gradient of 0.3 bar will be experienced at apogee, giving a total shear force of 924 N. A hole with a 3 mm diameter is drilled into the airframe to mitigate this environmental pressure gradient. The venting hole leads to a volume flow analysis to calculate the pressure buildup in the parachute bay. The pressure loss occurs much slower than the pressure gained during pressurization. See Appendix M for detailed calculations.

On the other hand, the shear screws can not be too sturdy, as this would prevent separation. Due to production delays, the final tests to decide the number and size of shear screws and the final pressure in the COPV are yet to be determined. Separation tests validating the system will be performed and documented before the 29th of September. However, earlier versions of the separation system have been flight-tested and validated in the two last projects. As a result, the separation test will provide the validation needed.

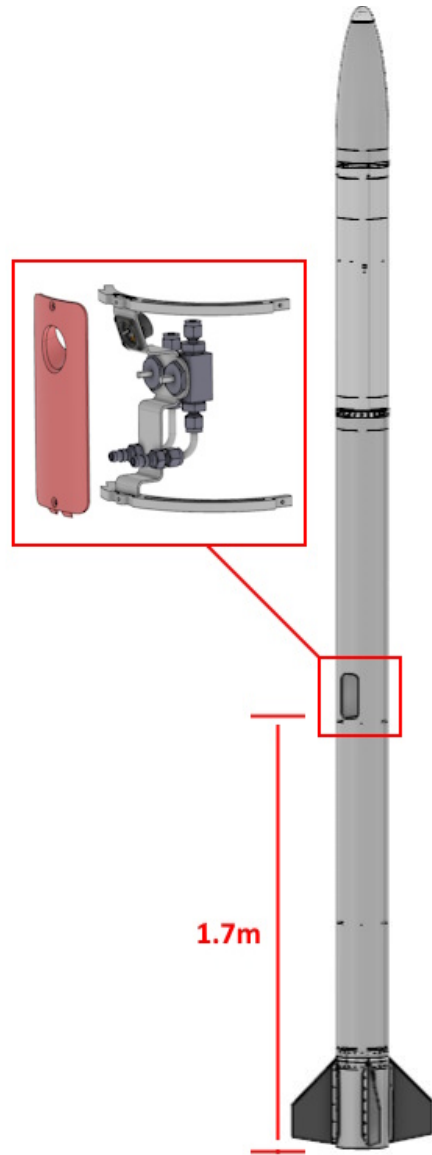


Figure 43: The filling valve is located 1.7 m away from the bottom of the boat tail, behind a hatch.

9.3 Deployment system

The deployment system consists of a drogue and a main parachute. The parachutes provide the rocket with a controlled descent after separation and secure a safe landing. The drogue parachute's primary function is to slow the descent from apogee and reduce drift until the main parachute is released at 400 m AGL. The main parachute's function is to slow down the descent rate to prevent damaging the rocket on ground impact. See the different flight phases in Figure 44.

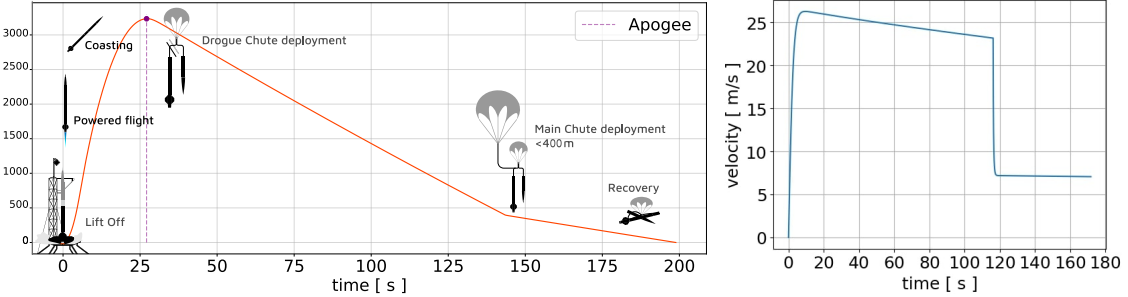


Figure 44: Flight phases and altitude over time (left), velocity over time, note $t = 0$ is apogee here (right).

This year's recovery team has designed and produced the drogue and main parachute in-house. The drogue parachute is designed to have a descent rate of 23 m/s a 65 kg dry mass. The drogue parachute descent rate determines the deployment force from the main parachute. The low descent rate, therefore, allows the main parachute to be larger, thus lowering the descent rate to 7.07 m/s, which complies with E3.1.2, with an expected deployment force of 6693 N.

The designs are based on the parachutes from *Fruity Chutes* and the *Parachute Recovery Systems Design Manual* by *Theo W. Knacke* [4]. The parachutes are designed with a minimum safety factor of 2 and use military-grade materials from *Paragear* such as rip-stop nylon for the canopy and nylon cords for the shroud lines.

Figure 45 illustrates the deployment system configuration. During decent under drogue, the main parachute is packed inside a parachute bag (pink) to contain it and to house the shock chords and shroud lines. This bag is then encapsulated by a cover bag (green) to make sure the main parachute does not have an early deployment and to decrease the risk of entanglement with the shock chords and shroud lines. This cover bag has its opening on the bottom and has a locking mechanism that closes the bag and is attached to the main chute release mechanism. The cover bag won't open unless the main chute release mechanism is activated. The drogue parachute is connected to the rim of the venting hole of the main parachute, so when the primary chute release mechanism is activated, the drogue pulls on the main parachute to deploy it.

The deployment system also has several features that improve its performance and robustness. One feature is a metal ring that is used to delay the opening of the main parachute, effectively reducing the opening shock. Another feature is shock cord reinforcements that minimize the chance of wear and tear on the shock cords when in contact with the airframe. Figure 46 shows two examples of previously used shock cord reinforcements. For further details of the deployment system, see Appendix G

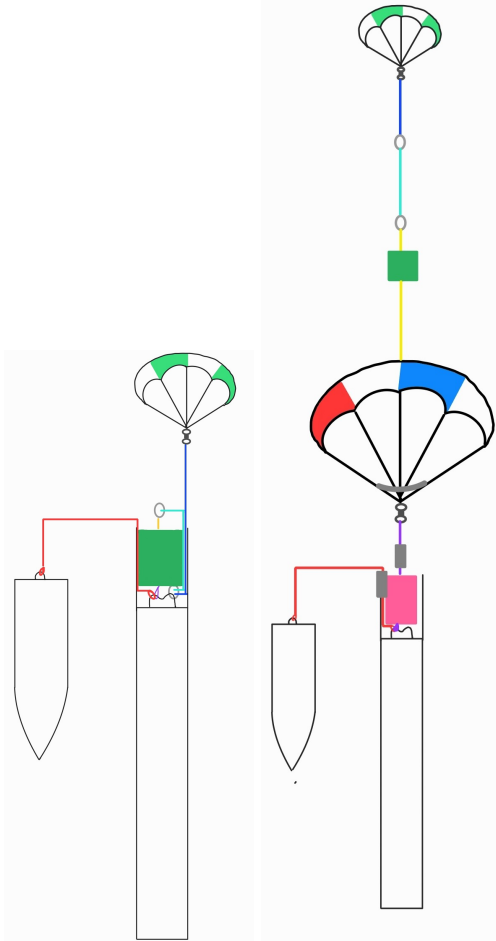


Figure 45: Deployment configuration.



Figure 46: A tennis ball used on project Stetind (left) and leather used for project Birkeland (right).

9.4 Main chute release system

The MCRS is a mechanism with the primary function of deploying the main parachute. An overview of the mechanism is illustrated in Figure 47. At 400 m altitude AGL, the FC will activate one of the servo motors belonging to the MCRS. The motor pushes the release arms, deploying the main parachute. The MCRS features two servo motors, an upper-release arm, and a lower-release arm mounted to two steel plates. In addition, a quick link connected to a shock cord retains the main parachute and the drogue parachute by locking it between the upper release arm and the steel plates. MCRS functions are illustrated in Figure 48. Note that there are two servo motors, one connected to the SRAD FC and the other to the COTS FC, making the system electronically redundant.

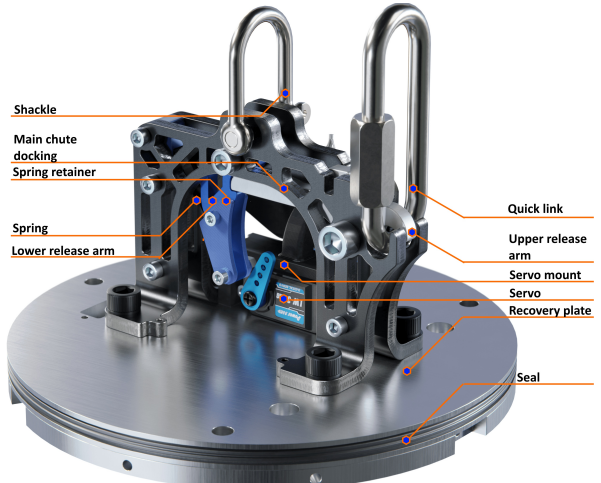


Figure 47: Overview of MCRS.



Figure 48: MCRS locked position (left), MCRS actuated (right). Note that one of the two servos is hidden to display the mechanism more clearly.

Another function of the MCRS is to be a fastening point between the forward airframe and the drogue parachute. When a load is applied to the system, rotation of the upper release arm is prevented by the lower release arm. A higher load implies that a higher force is needed to rotate the lower release arm to deploy the parachute. The parachute bag is also retained by MCRS, effectively reducing the risk of early deployment, which has been an issue for the past two projects. Another risk is that the system is not mechanically locked when no load is applied to the quick link. Because of heavy vibrations during ascent, the release arm can vibrate out of its position. As a mitigation, a spring is installed to keep the arms in place.

The system is designed for ease of manufacturing. The parts have been produced with laser cutting technology from 6 mm steel plates of type S650MC. Then, the bending process turns the main chute docking 90° to its wanted shape. Laser cutting is automated, while bending is a simple manual operation. Both operations are cost-effective and streamline system production.

The system has been verified using FEA. For the system to function correctly, it cannot experience any significant deformation. This could result in components jamming and prevent the release of the main parachute. Therefore, the chosen material is high-strength steel, S650MC—the high strength results in sufficient safety factors.

Moreover, the recovery hardware consists of a recovery plate that connects the MCRS to the inner structure and airframe and a coupler connecting the forward airframe to the nosecone. The validation of these parts can be found in Appendix M. The safety factors and loads are summarized in Table 17. Note that the coupler is glued to the nosecone and overlaps one diameter with the forward airframe.

Table 17: Summarized results from FEA

Part	Worst case load [N]	Experienced stress [MPA]	FoS
Upper release arm	2210	292	2.2
Lower release arm	2210	228	2.9
Main chute docking	5670	320	2.0
Recovery plate	5670	226	1.2 ¹
Coupler	10.3 and 4.21Nm	0.205	1009 ²

¹ Safety factor of 1,2 in tiny areas and neglectable see FEA-report.

² High safety factor against yield. Thickness is limited by the material available and the cost of production.

9.5 Deployment forces

The deployment forces were calculated using the drag force equation,

$$F_D = \frac{1}{2} \rho v^2 C_D A. \quad (1)$$

The calculations were calculated with a Python script using the equation mentioned above. For more details see Appendix M Parachute Calculations and Trajectory Simulations. Table 18 shows the results and corresponding safety factors. A safety factor of a minimum of two was targeted.

Table 18: Overview COTS components and experienced load.

Component (material)	Deployment stage	Experienced load maximum [N]	Rated maximum load [N]	Safety Factor
Main parachute (nylon) ¹	Main	5887	13341	2.3
Drogue parachute (nylon) ¹	Initial	2222	5280	2.4
Quick link (Stainless steel)	Main	6693	17795	2.7
Swivel link (Stainless steel)	Main	6693	18639	2.8
Shock chords (Nylon)	Main	6693	13341	2.0
U-bolt	Main	807	8896	11.0
Shackle	Main	6693	13734	2.1

¹ Rated maximum load listed is weakest part of the respective parachute.

10 Avionics

10.1 System Overview

The avionics system of Bifrost consists of two central systems: the recovery avionics system and the engine avionics system. Bifrost uses the CATS Vega as a COTS flight computer, which is connected to two servos for deploying the recovery system. The SRAD recovery avionics of Bifrost uses an accelerometer and a barometer to detect the apogee for deploying the drogue chute and determine the altitude for deploying the main chute. The two systems and a camera are connected to the Radionor CRE2-144-LW transceiver through an Ethernet switch. Additionally, two GNSS antennas are connected to the SRAD flight computer. These antennas are positioned separately from the noisy electronics, such as recovery servos and switching regulators, to ensure the best possible signal.

The power system for Bifrost is separate from the recovery and engine avionics systems, each featuring a dedicated spot-welded lithium-ion battery pack and SRAD Battery Management System (BMS). The COTS avionics is powered by its own lithium-ion battery pack to ensure redundancy. Both the recovery avionics BMS and propulsion avionics BMS are charged by the same umbilical cord, facilitating infinite standby time for the SRAD system. The umbilical cord detaches upon launch, and the BMS switches to battery power. The avionics are armed using two magnetic switches in the forward airframe for COTS and SRAD and one in the aft airframe for the propulsion avionics.

10.2 COTS Avionics System

COTS avionics is included in the rocket's recovery system to ensure a proven and redundant system of electronics onboard. CATS Vega is chosen as the COTS flight computer as it is required by EuRoC [1]. Table 20 shows the technical specifications of each component in the COTS avionics system. A diagram of all connections of the COTS avionics system is found in Figure 49. The COTS avionics system has a battery dimensioned for extended pad standby. Battery specifications and estimated on-time are provided in Table 19.

Table 19: COTS battery system specifications

2S1P Li-ion battery	
Continuous current consumption	110 mA
Maximum current consumption	4710 mA
Nominal battery voltage	7.4 V
Battery Capacity	8900 mAh
Estimated battery life	81 hours

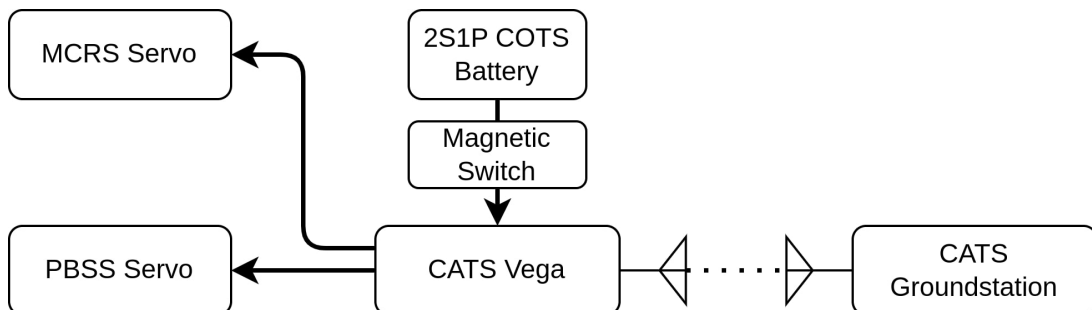


Figure 49: Overview of COTS avionics system.

Table 20: COTS component overview.

Component	Nominal voltage [V]	Max current consumption [mA]
CATS Vega	7 - 24	100
PBSS Servo (PowerHD LW-30 MG)	4.8 - 7.4	2300
MCRS Servo (PowerHD LW-30 MG)	4.8 - 7.4	2300
Mag. Switch (Featherweight)	3.5 - 16	0.007
2S1P Battery (8900 mAh)	7.4	N/A

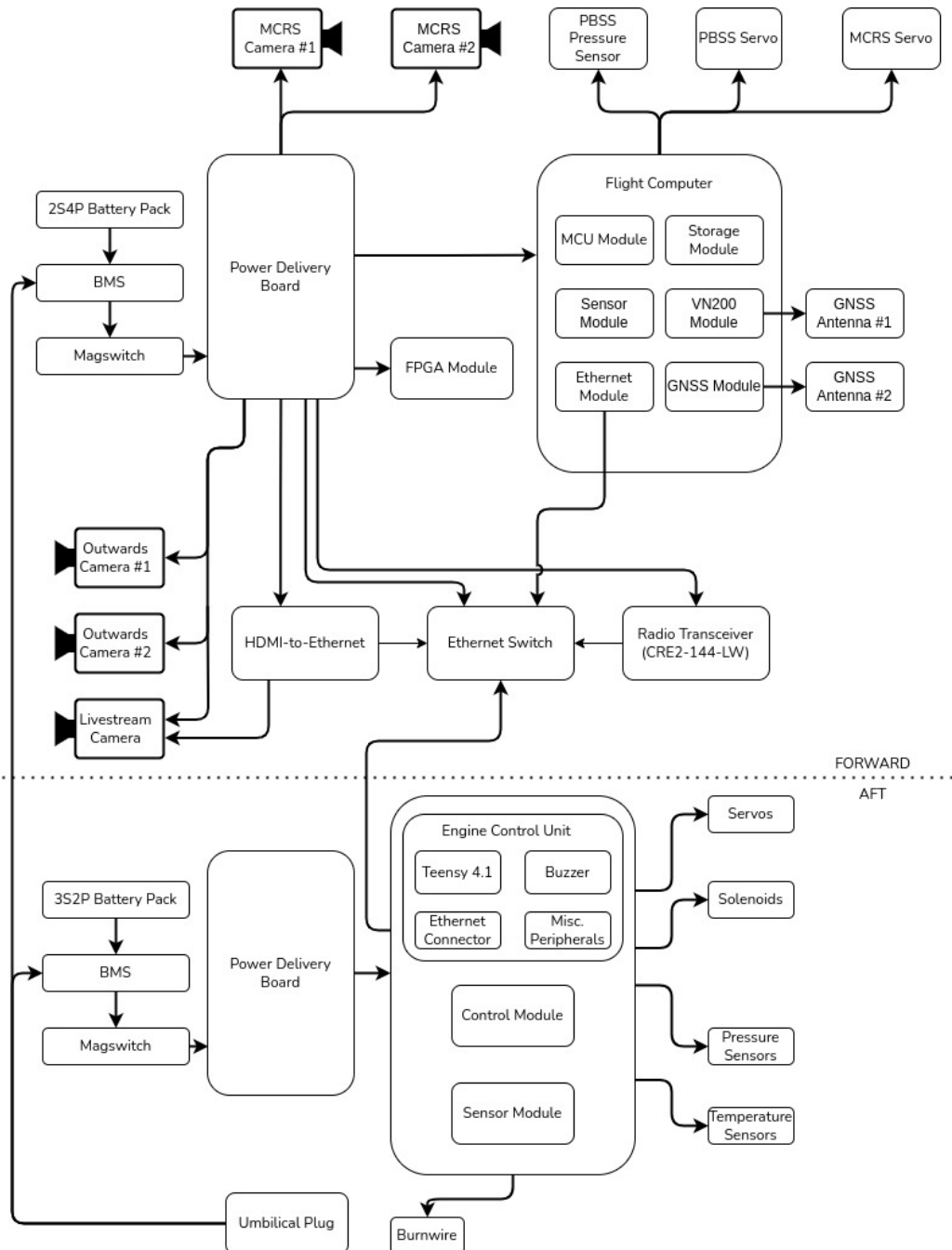


Figure 50: Simplified SRAD electrical system overview.

10.3 SRAD Electrical System

The SRAD electrical system consists of multiple subsystems. The SRAD Flight Computer (FC) is the forward airframe's central unit, while the aft's central unit is the SRAD Engine Control Unit (ECU). Both of these units communicate with the ground station through an ethernet switch, which is connected to the onboard radio transceiver.

A BMS is developed to provide power to all subsystems. The forward and aft airframe has its own BMS controlling separate battery packs. The SRAD BMSs provide standby power to the rocket while it is at the pad and handle cell balancing of the batteries. It also can monitor the battery pack's voltage, current, and temperature levels.

The rocket also has five cameras, consisting of three outward-facing cameras, including one for live video streaming. The two others are placed in the recovery bay to capture separation and main chute release. Figure 50 shows a simplified electrical system overview.

10.3.1 Flight Computer

The SRAD flight computer shown in Figure 51, is of a modular design. This design allows for the reuse of previous modules and easy replacement of damaged modules during or before launch operations. A rendering of the flight computer is shown in the figure below. The SRAD flight computer consists of eight modules, each with functionalities described in the table below.

Table 21: Flight computer module functions.

Module	Function	Main Components
Microcontroller	Houses the microcontroller module, which controls the FC	STM32H753ZIT6
Ethernet	Integrates the Ethernet transceiver and RJ45 port for telemetry	LAN8742A
Sensor	Integrates barometer, accelerometer, IMU, magnetometer, and humidity sensor	MS5607, IIM42652, LIS3MDL, H3LIS331DL, BME280
VN-200	Integrates the VN-200 sensor suite module	VN-200
NEO-M9N	Integrates the GNSS module for positioning	NEO-M9N
Storage	Integrates storage solutions for the FC	SD-card holder and S25FL512



Figure 51: Rendering of the Flight Computer.

Continued on next page

Table 21 : Flight computer module functions. (Continued)

XBee	Integrates an XBee module (only for testing)	XBee Pro S3B
------	---	--------------

10.3.2 RF System

The rocket utilizes a CRE2-144-LW radio transceiver to allow for telemetry between the ground station and the rocket. This radio has been flown twice and has a tested range farther than 25 km. It also allows for an HD camera feed during flight, allowing for event detection. All transceivers/receivers are described in Table 22.

Table 22: Overview of antennas used

Device	Antenna type	Operating frequency	Intended use
Radionor CRE2-144 LW	Monopole whip	4.9 - 5.9 GHz	Communication with ground station, transmitting data and video feed
CATS Vega	Happymodel ELRS Moxon	2.4 GHz	Transmission of COTS FC data
CATS Vega	APAE1575R1820ABDC1-T patch	1.575 GHz	Receive GNSS signals
VN200 and NEO-M9N	2× AS-ANT2B-ANN patch	1.559 - 1.606 GHz	Receive GNSS signals

10.3.3 Engine Control Unit

The engine control unit (ECU) shown in Figure 52, is the central part of the propulsion avionics system. The ECU consists of three main modules: The sensor module, the control module, and the carrier board. It utilizes the Teensy 4.1. module for ease of programming as it supports prewritten Arduino libraries. It uses Ethernet to communicate with the radio. Table 23 below shows the functionality and essential components of the modules.

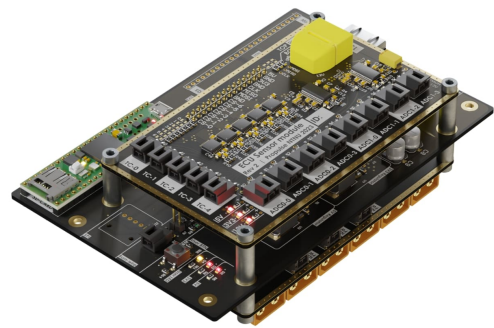


Figure 52: Rendering of the Engine Control Unit.

Actuators

The propulsion system uses servos and solenoids to actuate the valves. Table 24 below shows an overview of all actuators used. The control board implements a high-side load switch for servos and solenoids, enabling power control to the actuators.

Sensors

For monitoring the propulsion system, pressure sensors and thermocouples are used. Table 25 shows the sensors used.

Table 23: ECU module functions.

Module	Function	Main Components
Carrier Module	Connects the two modules, and houses the Teensy 4.1	Teensy 4.1
Sensor Module	Handles output from pressure transducers and thermocouples as well as supplying pressure transducers with power	ADS8678 and MAX31856
Control Module	Interface to the solenoids and servos in the propulsion system	VN5E050 Load-switch

Table 24: Actuators used in the propulsion system.

Actuator	Function	Actuator Type	Input Voltage [V]	Speed	Torque [kg/cm]	Max current draw [mA]
Power HD T70-12V	Main OX Valve Main Fuel Valve Pressurizing Valve OX filling valve Purge valve	Servo	8.4 - 12.6 V	0.10 °/s @12 V	75 kg/cm @12 V	3300 mA
Jaksa 327714	OX Vent Fuel Vent	Solenoid	24 V	N/A	N/A	750 mA

Table 25: Sensors used in the propulsion system.

Sensor	Sensor Type	Function	Input Voltage [V]	Output Voltage [V]	Range
PBT-RB060	Pressure transducer	OX Tank OX Injector Fuel Tank Fuel Injector Chamber	8-30 V	0-5 V	0-60 bar (relative)
PBT-RB400	Pressure transducer	N2 Tank	8-30 V	0-5 V	0-400 bar (relative)
Thermafühler Screw-in thermocouple	Type K thermocouple	OX Tank Top OX Tank Bot OX Injector Fuel tank Fuel Injector	N/A	N/A	-100 to 1100 °C

Ignition Detection

The propulsion system uses a solid rocket motor for ignition. This makes the system compatible with EuRoC's fire control system. To detect the igniter's activation, a small burnwire is carefully placed in front of the solid rocket motor before inserting the igniter. When this burnwire is burned, the ECU detects a loss in continuity, and the ignition sequence commences. A series of conditions must be met during this ignition sequence to ensure nominal startup.

10.3.4 Arming System

Arming of the SRAD and COTS avionics is done through their own respective Featherweight magnetic switch. The arming procedure will consist of moving a sufficiently sized magnet across the vicinity of

the magnetic switch. The magnetic switches are placed in the recovery module shown in Figure 31 and the nitrogen module shown in Figure 37. Therefore, Arming the avionics in the recovery module requires a ladder. This is deemed safe as the rocket is inert when arming.

10.3.5 Camera System

The rocket is equipped with a total of five cameras, one of which is streamed to the ground station. The livestream camera has an HDMI interface, which can be streamed to the ground station through an HDMI-to-Ethernet encoder. Table 26 shows the specifications and tasks of the cameras.

Table 26: Camera specifications

Nr.	Camera model	Resolution	FOV °	Streamed	Task
1	HawkEye Herelink 4K60 EIS 4.0	3840×2160	170	Yes	Live event capturing
2	RunCam Split HD	2704×1520	170	No	Recovery post-launch analysis
3	RunCam Split HD	2704×1520	170	No	Recovery post-launch analysis
4	RunCam Split HD	2704×1520	170	No	Marketing and post-launch analysis
5	RunCam Split HD	2704×1520	170	No	Marketing and post-launch analysis

10.3.6 Power System

Power Budget

The power consumption of the electrical system is calculated and measured to determine the battery packs' size accurately. The power budget can be found in the power budget sections of Appendix J and Appendix O.

Batteries

The power system utilizes Samsung 18650 lithium-ion battery cells. As per requirement by [1] 3.5, these cells are encased by a metal cylinder. The cells will be spot-welded, to ensure proper connection. The battery's specifications are in the following table below.

Table 27: Battery specifications.

Battery pack	Name	Configuration	Nominal voltage [V]	Max discharge current [A]	Typ. capacity [mAh]
Recovery	INR18650-35E	2S4P	7.4	32	13800
Propulsion	INR18650-20S	3S2P	11.1	60	4000

Battery Management System

The battery management for Bifrost is designed to handle the charging, cell balancing, and monitoring of the batteries. See the Appendix J for more information.

DC-DC Regulators

The system uses low dropout regulators and boost regulators to power specific devices within the rocket. These regulators are housed on the forward and aft airframe power delivery board. See the table below for the required regulators that are housed on the power delivery boards.

Table 28: Regulators used.

Voltage	Component(s)	Regulator	Type	Max current draw [mA]	Regulator max current [mA]
12 V	CRE2-144-LW PBSS Pressure Sensor Hawkeye Camera	U3V70A	SMPS	2730	4000
				20	
				300	
5 V	RunCam Cameras HDMI-to-Ethernet	MIC29502WU	LDO	1800	5000
				200	
24 V	Solenoids	U3V50F24	SMPS	1500	2500

Umbilical Solution

An umbilical cord enables on-pad charging until launch, where it easily detaches. The umbilical cord connector chosen is the RoPD by Rosenberger connector, which has a 25 A max current load and one-directional functionality.

10.4 SRAD Software System

The SRAD software system is designed to provide robust control and communication for safe operation. The software operates primarily through two central units: the SRAD Flight Computer Software for the recovery and telemetry and the SRAD Engine Control Unit Software for managing actuators related to the engine.

10.4.1 Flight Computer Software

The SRAD Flight Computer software's main functionality is activating the recovery system and gathering, transmitting, and storing data about the rocket's state during flight. Table 29 shows the tasks run on the flight computer to ensure the main functionality is fulfilled. The tasks are run on an STM32H753ZIT6 as individual threads using Azure RTOS. More information about the recovery software Appendix I.

Table 29: Flight Computer tasks

Priority	Subsystem / Task	Description
1	Finite state machine	Update Finite State Machine (FSM) based on the estimated altitude and activate actuators if the activation criteria are met.
2	State estimation	Filters sensor values and uses this data to estimate altitude.
3	Sensor sampling	Reading sensor values
4	Storage	Stores raw sensor values, filtered values, estimated altitude, FSM state, and timestamps for post-analyses.
5	Telemetry	Transmit raw sensor values, filtered values, estimated altitude, FSM state, and timestamps for a live status report of the rocket.

Finite State Machine

The FSM divides control of the rocket during different stages of flight into smaller and more manageable states. The states are Initialization, Idle, Armed, Powered, Coast, Drogue chute, Main chute, and Retrieval, each responsible for slightly different tasks. A visualisation of these states and their occurrence during flight is shown in figure 53. The state machine will operate linearly, with no possibility of retracing its steps into a previous state, ensuring the system will not fail unexpectedly.

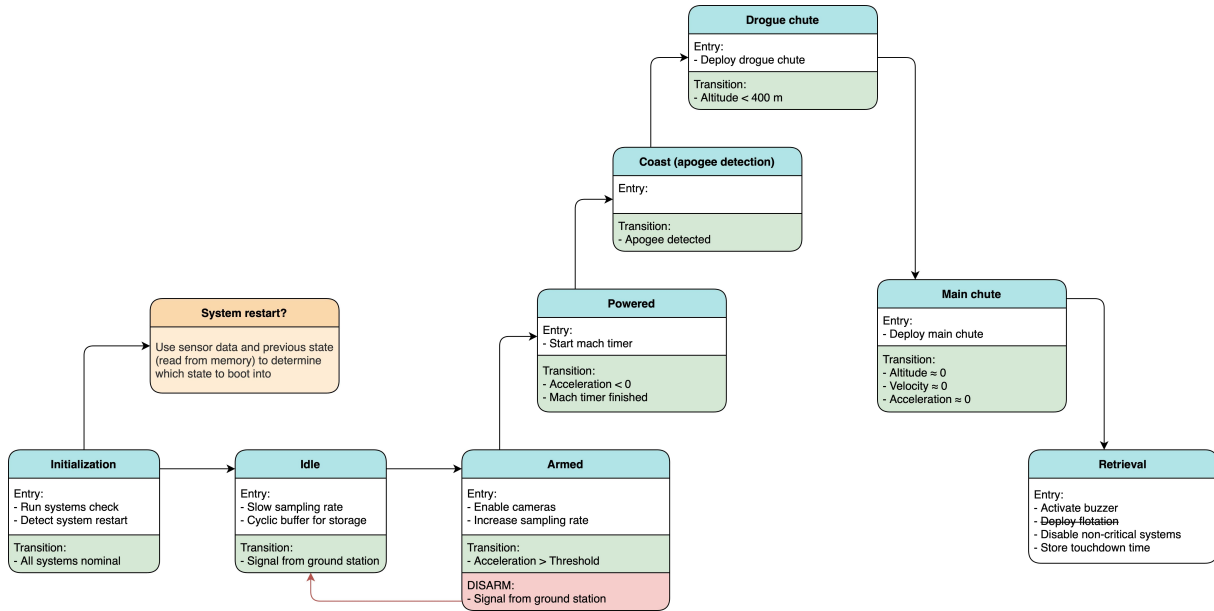


Figure 53: FC FSM

State Estimation

The SRAD flight computer uses an Extended Kalman filter, similar to the COTS flight computer, to estimate four physical variables: height, velocity, acceleration, and acceleration bias. The initial values of these states are set to zero and are calculated using data from one of the accelerometer axes and a barometer. The Kalman filter assumes that the rocket always points vertically or that the angle does not change significantly during the idle, powered, and coast phases.

Sensor Sampling

The rocket features a wide variety of sensors, some of which are mission-critical and some of which are not. Sampling of all sensors will happen at up to 100 Hz and is a highly prioritized task, as all the other subsystems require functional sensor data to perform as expected. It is possible to categorize the different sensors into groups based on their importance; our barometer and IMU are mission-critical and classified as navigational sensors, while others are present for post-flight analysis and classified as miscellaneous.

Storage

During the flight, a 64 MB flash chip will be employed for sensor data, state estimations, and FSM data. The telemetry thread will transfer these data into a ring buffer. The storage thread will remain in a standby state, awaiting the buffer to accumulate a minimum of 512 Bytes of data. Once this threshold is reached, the contents of the buffer will be saved to the flash memory. As a contingency plan, SD card storage should be an alternative option if flash memory fails to function.

Telemetry

The telemetry subsystem comprises a single thread transmitting data from the FC to GS. The UDP protocol will send this as Ethernet packets from the FC to the radio. Azure RTOS NetX functionality was chosen over the lightweight IP stack because of its superior compatibility with the rest of the RTOS.

Data processing occurs on the GS to preserve computational power on the FC. All data is sent as raw bytes. With fixed positions assigned to the different sensors in the data frames, the only overhead is the data needed for the Ethernet protocols.

10.5 Engine Control Unit Software

The engine control software manages vital functions, including sensor data collection, valve control, ground station telemetry, and onboard data storage. It employs a C++ codebase developed with PlatformIO and Teensyduino for enhanced efficiency and flexibility. More information about the engine control unit software can be found in Appendix O.

Structure

The ECU software operates within a structured task framework, utilizing a primary finite state machine to oversee the filling and launch processes. This state machine ensures valves' correct positioning and rocket operations' safety. Detailed FSM information is provided in the appendix. Supplementary tasks include sensor sampling and ground station communication.

Sensor sampling and telemetry

Two sensor types are employed: pressure sensors and temperature sensors, each with distinct sampling requirements. Pressure sensors are sampled during program idle periods to detect system instabilities. Temperature sensors are tested at a fixed 9Hz rate due to TDC conversion time constraints. Data is buffered and subsequently stored on the onboard SD card and transmitted via UDP sockets to the ground station. Additionally, the ECU sends status updates, debug data, and accepts ground station commands, allowing for manual state machine control during filling.

10.6 SRAD Ground Station

The ground station and telemetry system have functions that can be seen in a prioritized order in Table 30. More information about the ground station and telemetry system can be found in Appendix H.

Table 30: Groundstation functions

Priority	Function	Description
1	Send change state / disarming signal	Arming and disarming the rocket remotely
2	Receive, store and display telemetry	Store and display all telemetry
3	Tracking the rocket	Using the radio to track the direction of the rocket reliably
4	Video stream and documentation	Store, display, and stream live video from the rocket

10.6.1 Ground Station Hardware

The ground station uses Radionor's CRE2 system, operating at the 5 GHz band, offering a 25 km signal range and 7 Mbps data rate. This supports HD video and telemetry. Equipment includes CRE2-144-LW onboard for rocket communication and CRE2-189 for ground station. The CRE2-189 is a high-gain phased array placed on a tracking mount to allow active rocket tracking.

10.6.2 Ground Station Software

CRE2 radios enable IP routing and will be pre-assembled on the network. UDP will be used for efficient telemetry and video streaming. Telemetry data is managed by a ground station Python server. The React-based GUI facilitates real-time telemetry monitoring, rocket control (arming, disarming, camera control), and propulsion system state changes during filling.

10.6.3 Ground Station Tracker

The radio tracker operates on the open-source ROS framework, ensuring it meets the performance requirements detailed in the telemetry appendix, with a built-in safety margin. The system employs two

stepper motors with drivers to execute robotic movements and track the rocket vertically and horizontally from the ground. The CRE-189 radio is mounted on an SRAD assembly, controlled by a Rock Pi, which manages the tracking software as a finite-state machine. The tracker follows a modeled trajectory during ascent, transitioning to radio signal vector positioning post-ascent. Manual control is available in case of system malfunction.

11 Payload

11.1 Introduction

The BioSat is a nano-satellite project currently being developed by Orbit NTNU. Its mission is to study the growth of biological material in a low-earth orbit. The project consists of many new designs that require extensive testing. Therefore, the payload's main objective is to test the functionality and reliability of the BioSat prototype in a high acceleration/vibration environment. The different subsystems that Orbit NTNU aims to test are: Solar panel deployment mechanism, solar cell durability, OBC reliability, Biobox strength and environment stability, growth agar durability, seed deployment mechanism, and 3U frame strength.

11.2 Payload structure

The payload structure consists of a 3U frame produced at NTNU. The satellite bus inside the 3U satellite consists of 2 PCBs, EPS and OBC. There will also be an early prototype of the Biobox, the atmospheric chamber containing a plant shown in figure 54. The solar panels will be mounted on the outside of the 3U frame.

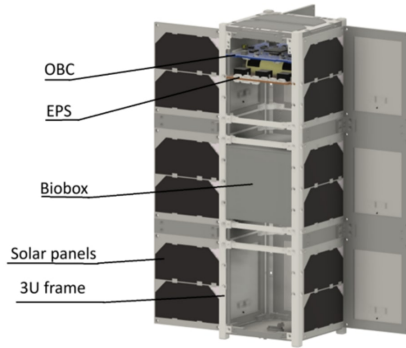


Figure 54: Overview of BioSat and included sub-systems

11.3 BioBox

The Biobox is the container that contains the organic material being grown. The box consists of an airtight metal container containing several sensors, a cable feedthrough, growth agar, and the seed deployment mechanism. The plant will be grown in an agar medium. It is designed to provide plant nutrition and water in a gravitation-free environment without complex watering/feeding mechanisms. Testing the reliability of the agar in a realistic launch environment will provide valuable data that can be used to improve the reliability of the final product. The Biobox enclosure's function is to protect the plant from the external space environment. The container will include sensors to measure pressure, temperature, humidity, and acceleration. The data from these sensors will be used to measure the environmental stability the Biobox provides.

11.4 Electronics

The electrical system of the payload consists of EPS, OBC, and BioBox electronics. EPS is short for Electrical Power System and contains the batteries and voltage regulators. The EPS uses two 18650 Lithium-ion batteries with internal protection with a total battery capacity of 7000mAh. It also includes the Payload's Remove Before Flight (RBF) connector to activate the payload before launch. The Biobox contains several sensors to measure the environmental conditions inside the Biobox and send the data to the onboard computer (OBC) through an I2C interface. The OBC is the processor that saves the data to an SD card and controls the payload through an STM32 microcontroller.

Orbit NTNU has also designed custom solar panels and a panel deployment mechanism. These modules must be reliable because premature deployment of the panels could result in a total mission failure. The durability of the solar cells making up the solar panels is also being tested to ensure the launch vibrations do not damage them.

12 Conclusions

Project Bifrost strays from the traditional project scope of Propulse NTNU, with increased cost, complexity and ambitiousness, together with an increased team size and degree of multidisciplinarity. Since the beginning of the project, Propulse has been able to design, test, iterate and produce a flight-worthy liquid engine, all-the-while creating a robust rocket around it. Through this, the project has united a team of 80+ active members and mentors with an advancing Norwegian space-industry, motivating all of the involved to seek new and bigger challenges to partake in for the future. Due to the increase in complexity and ambitiousness, Propulse has had to improve on procedures for safety and testing of pressurized systems, documentation of complex systems, the gathering and allocation of resources, as well as the ability to delegate tasks across a broad team of members. Regardless of outcome at EuRoC, Project Bifrost has elevated both the technical and organizational level of professionalism and thoroughness, something that future projects will benefit from greatly.

Some of the key lessons learned are listed below:

- Things takes time – Include flexibility to account for unforeseen issues, and don't let the thought of a perfect system ruin your chance of launching with a less perfect design.
- Strive to get your system in hand – The more practical experience you get, the better you'll know the system, and the faster you can iterate.
- Clear goals, guidelines and requirements is key for managing a large team.
- Good business relations are essential, and must be conducted with similar preparation, effort, and care as the other aspects of the project.
- Working with pressurized systems can be dangerous, and the safety of all involved members must be taken extremely seriously.
- Give members responsibility and clear expectations early - more ownership to the individual member yields higher motivation

After the launch at EuRoC, the team will process all data and experiences gathered from the launch campaign to finalize the finished project documentation. This documentation takes the form of a extended technical report, and the contents of the report will be summarized and presented for the organization when done. The purpose of this is that the upcoming board and members are able to follow-up the progress done for Project Bifrost and build on that for future projects that will take Propulse NTNU closer to the goal of space.

Propulse's next project started on September 8th 2023, and will carry on the torch from Project Bifrost. The goal of Project 2024 is to launch and return a payload to 10 000 m with a bi-liquid rocket, and with that leave behind a robust and intuitive platform for bi-liquid sounding rockets, such that future board members can understand and develop the technology and organization even after the current members have graduated.

Remaining design challenges to be tackled are as follows: balancing the performance and cooling capacity of the regeneratively cooled combustion chamber, being able to operate the main propellant valves of the propulsion system in a repeatable and controlled fashion across a wider range of operational conditions, and creating a design that ensures efficient operation and handling before launch.

Areas of improvement uncovered during the project is the ability to ensure ownership across all member of the project, as well as the ability to ensure transfer of knowledge regarding not only the result, but also the process of conducting a project, and that on all organizational levels.

Acknowledgements

Thanks to all participating members on the Bifrost project:

Simen Flåtter Flo <i>Project Manager</i>	Vegard Sund <i>Inner Structure Engineer</i>	Martin Salthé <i>Embedded Software Engineer</i>
Mikkel Gisleberg <i>Deputy Project Manager</i>	Vebjørn Gulbrand Bratlie <i>Recovery System Lead</i>	Simen Kartveit Bjerkstrand <i>Navigation System Engineer</i>
Even Drugli <i>Chief Technical Officer</i>	Hege Grytten <i>Recovery System Engineer</i>	Ola Flaata <i>Ground Station and Telemetry</i>
Trygve Nummedal Os <i>Chief Marketing Officer</i>	Johannes Eiriksønn Mørkrid <i>Recovery System Engineer</i>	Maya Saint-Victor <i>Ground Station Engineer</i>
Harald Bjerkeli <i>Software R&D Lead</i>	Kasper Michat Zajac <i>Feed System Lead</i>	Mori Adrian Rosland <i>Embedded Software Engineer</i>
William Dugan <i>Chief Propulsion Engineer</i>	Ulrik Garmark Anker <i>Feed System Engineer</i>	Stian Alseth <i>Propulsion Avionics Lead</i>
Trond Steinagard <i>Combustion Chamber Lead</i>	Tom Rathjens <i>Feed System Engineer</i>	Abel Horneland <i>Test Software Engineer</i>
Brage Bang <i>Combustion Chamber Engineer</i>	Luis López Redondo <i>Feed System Engineer</i>	Mikkel Blomnes <i>Propulsion Electrical Engineer</i>
Ellen Katrine Krucksve <i>Combustion Chamber Engineer</i>	Andreas Ronglan <i>Feed System Engineer</i>	Gregor Moe <i>Propulsion Electrical Engineer</i>
Emil Fylling <i>Combustion Chamber Engineer</i>	Miguel Campos Moliner <i>Test Site Lead</i>	Even Hugdal <i>Videographer</i>
Iris Matre <i>Combustion Chamber Engineer</i>	Oscar Oddsen Arne <i>Test Site Engineer</i>	Theo Viken <i>Social Media Manager</i>
Karina Ovedal <i>Combustion Chamber Engineer</i>	Sverre Ose Kristensen <i>Cheif Avionics Engineer</i>	Ellinora Gjerde <i>Graphical Designer</i>
Krystian Chmielarski <i>Combustion Chamber Engineer</i>	Martin Eggen <i>Electrical Lead</i>	Ola Vanni Flaata <i>Head of Mission Control</i>
Naglius Kirvaitis Brandal <i>Combustion Chamber Engineer</i>	Martin Færavaag <i>Electrical Engineer</i>	Ane Kristine Havstad Morkemo <i>Mission control</i>
Robert Kalrud <i>Chief Mechanical Engineer</i>	Sondre Skjelland <i>Electrical Engineer</i>	Thanathon Holm <i>Mission Control</i>
Henrik Ross Gobakken <i>Outer Structure Lead</i>	Kristoffer Bjerkvik <i>Electrical Engineer</i>	Tobias Ringedalen Thrane <i>Web Developer</i>
Endre Ekstang Grønevik <i>Outer Structure Engineer</i>	Trygve Jørgensen <i>Electrical Engineer</i>	Daniel Jiangdi Gou <i>Technical Writer</i>
Jonas Mårvad Øvstegård <i>Outer Structure Engineer</i>	Filip Kristoff <i>Embedded Software Engineer</i>	Johanne-Marie Talberg Andersen <i>Logistics Manager</i>
Thomas Forberg Haugvaldstad <i>Inner Structure Lead</i>	Mathias Otnes <i>Embedded Software Engineer</i>	Anders Kristensen <i>Web Developer</i>
Sigurd Malmin Hansen <i>Inner Structure Engineer</i>	Theodor Johansson <i>Embedded Software Engineer</i>	Anders Hestad <i>Renders & Electrical</i>

The team thanks our alumni mentors for feedback and guidance throughout the project:

Svein Jostein Husa
Avionics Mentor

Rannveig Marie Færgestad
Propulsion Mentor

Steven Xu
Board Mentor

Rizqi Fairuz Wahyudin
Avionics Mentor

Einar Bergslid
Mechanical Mentor

Tea Christiansen Rasmussen
Board Mentor

Andreas Fanebust
Avionics Mentor

Tobi Heinz
Mechanical Mentor

Halvor Bakke-Veiby
Board Mentor

Jonas Trygve Aannestad
Propulsion Mentor

Arve Tokheim
Technical Mentor